# CANMET

Canada Centre for Mineral and Energy Technology

Centre canadien de la technologie des minéraux et de l'énergie

**Efficiency and Alternative Energy Technology Branch**

**Direction de la technologie de l'efficacité énergétique et des énergies de remplacement**

Energy, Mines and Resources Canada

Énergie, Mines et Ressources Canada

Canada

THE ENERGY OF OUR RESOURCES · THE POWER OF OUR IDEAS

L'ÉNERGIE DE NOS RESSOURCES · NOTRE FORCE CRÉATRICE

91-01234/

# ENHANCEMENT AND APPLICATION OF PV SYSTEMS SIMULATION PACKAGE: PHASE III

**PREPARED FOR:**

Efficiency and Alternative Energy Technology Branch
Energy, Mines and Resources Canada
Ottawa, Ont.
DSS Contract No. 66SS.23283-7-6130
March, 1990

**PREPARED BY:**

Electronic Devices Technology Group
Ortech International
2395 Speakman Drive
Mississauga, Ont.
and
TdS Dixon Inc.

**SCIENTIFIC AUTHORITY:**

Jimmy Royer
Efficiency and Alternative Energy Technology Branch
Energy, Mines and Resources Canada
580 Booth Street
Ottawa, Ont.
K1A 0E4

MICROFICHE

**CITATION**

Savage, J., P. Bruyn, O. Caporaletti, Electronic Devices Technology Group, ORTECH International and S. Dixon, TdS Dixon Inc. Enhancement and Application of PV Systems Simulation Package: Phase III. DSS Contract No. 66SS.23283-7-6130. Efficiency and Alternative Energy Technology Branch, Energy, Mines and Resources Canada, Ottawa, Ontario. 1990 (64 pp.)

Copies of this report may be obtained through the following:

Efficiency and Alternative Energy Technology Branch
CANMET
Energy, Mines and Resources Canada
580 Booth Street, 7th Floor
Ottawa, Ont.
K1A 0E4

or

Document Delivery Service
Library and Documentation Services Division
CANMET
Energy, Mines and Resources Canada
562 Booth Street
Ottawa, Ont.
K1A 0G1

© Minister of Supply & Services Canada 1990
Catalogue No. M91-7/102-1990E
ISBN. 0-662-18107-7

## Acknowledgements

We are grateful to Mr. D. Shipley of the Watsun laboratory, University of Waterloo, for his role in the work described in this report and in particular, the writing of portions of the final battery model description.

The interest and support of Mr. J. Royer, scientific authority for this contract, is also acknowledged.*

*This report is distributed for informational purposes only and does not necessarily reflect the view of the Government of Canada nor constitute an endorsement of any commercial product or person. Neither Canada nor its ministers, officers, employees or agents makes any warranty in respect of this report or assumes any liability arising out of this report.

TABLE OF CONTENTS


Abstract..... vi

Executive Summary..... 1

Résumé..... 5

1. Introduction..... 8

2. Objectives..... 9

3. Model Development for Non-Hybrid Control Strategies..... 10
3.1 Enhancement of PV Array Model..... 11
3.2 Enhancement of Battery Model..... 15
3.2.1 Overview..... 15
3.2.2 Battery Discharge..... 19
3.2.3 Battery Charge..... 21
3.2.4 Temperature and Current Dependence..... 23
3.2.5 Convergence Procedures..... 24
3.2.6 State of Charge..... 24
3.2.7 Reduction of Time Step Size..... 25
3.3 Addition of Several Control Modes..... 26

4. Comparison of Non-Hybrid Control Strategies..... 28
4.1 General Approach..... 28
4.2 Results and Conclusions..... 28
4.2.1 Base Case..... 28
4.2.2 Reduced Array Size..... 29
4.2.3 Undersized Array and Upsized Battery..... 29
4.2.4 Detailed Analysis of Results..... 33

5. Development and Implementation of PV-Diesel Model..... 36
5.1 Diesel Generator Requirements..... 37
5.1.1 Generator Capacity..... 37
5.1.2 Generator Start/Stop Conditions..... 38
5.2 Converter Requirements..... 39
5.3 AC Load Requirements..... 40
5.4 Input Specifications..... 40
5.5 Printout Additions..... 42

6. Development and Implementation of
Lead-Acid Aging Model..... 44
6.1 The Process of Aging..... 44
6.2 The Aging Model..... 46
6.2.1 Cycle Life Component of Aging Model..... 47
6.2.1.1 Implementation of the Cycle Life Component..... 51
6.2.2 Gassing (Electrolysis) Component of the Aging Model..... 52

6.3 WATSUN-PV Aging Model Input..... 53
6.4 WATSUN-PV Aging Model Output..... 54
6.5 Proposed Incorporation of Temperature Effects..... 55

7. Application of New PV-Diesel and Aging Models Using WATSUN-PV..... 56
7.1 Application of Aging Model..... 56
7.2 Application of PV-Diesel Model..... 58
7.2.1 Flat Load Profile..... 58
7.2.2 Irregular Load Profile..... 59

8. Conclusions..... 61

9. Recommended Future Work..... 62
9.1 Recoding in Pascal..... 62
9.2 High Accuracy Battery Characterization..... 62
9.3 Battery Testing for Aging Models..... 63
9.4 PV-Diesel Model Application and Next Version..... 63

References..... 64

## Abstract

This report describes the work carried out to extend and optimize the capabilities of WATSUN-PV, a simulation program for stand alone low power PV systems.

The effect of different system control strategies on system performance was studied. This required a significant enhancement of the existing PV array and battery models. Models for the addition of a diesel generator and for battery aging were also developed and implemented in the software.

No major differences in system performance were found due to the control strategy adopted. The choice of a particular strategy is thus an economic issue.

The new battery model is temperature sensitive and based on I-V characteristics. The aging model tracks the battery life reduction with use but does not modify the battery characteristics in the process.

The diesel generator was modeled by its capacity and the criterion for turning it on, based on the status of the rest of the system.

This work represents a significant enhancement to the capabilities of WATSUN-PV and its application as a simulation tool for stand alone low power PV hybrid systems. It is particularly suitable for the evaluation of systems operating under conditions of low insolation and low temperature like those found in locations in the Canadian North.

The need for further work in some areas is discussed and recommendations given.

## Executive Summary

Computer tools for the simulation of PV systems, operating under extreme conditions of low insolation, low temperature and remoteness, are required by users and designers of such systems for northern Canadian sites.

Ortech International in collaboration with the Watsun Group of the University of Waterloo and TdS Dixon Inc. has extended and optimized the capabilities of WATSUN-PV. This program can simulate and evaluate the performance of stand alone low power PV systems with battery storage.

The effects of different system control strategies, the addition of a diesel generator and battery lifetime on system performance were studied and models were developed for integration into what became version 3.0 of WATSUN-PV.

Remote northern Canadian sites are prime candidates for the widespread application of PV-diesel hybrid systems. However, questions of capital costs and reliability have not been totally resolved. The work described in this report contributes to the understanding of the interaction among the different components of hybrid systems and provides a tool to assess the performance of the overall system.

New models were developed for the PV array and the battery to support the implementation of five different control strategies and their comparison and to make WATSUN-PV simpler to use.

The new array model predicts hourly current and voltage conditions (I-V model) as a function of temperature and solar radiation. It also accepts module parameters which are available from manufacturers. The system control strategies that were studied were:

i) Maximum array power tracking with limiting battery voltage

ii) Maximum array power tracking with battery trickle charging

iii) Clamped array voltage with limiting battery voltage

iv) Clamped array voltage with battery trickle charging

v) Direct coupling between the array and the battery

The simplest way of comparing the various control strategies would have been to simulate them on five systems with identical component sizing, load requirements and meteorological data and then compare their performance. However, in practice the choice of one strategy over another one is based on economics. Therefore, the comparison was done by resizing each of the systems to yield the same performance in terms of reliability and load met. Any comparison between systems will then be based on the relative component sizing and the corresponding costs savings or penalties.

This iterative process is more time consuming but the results can be used directly in an economic analysis of the system.

The comparison of the five strategies was done for a remote site (Inuvik, NWT). The maximum power point tracked system required less storage. The trickle charger did not make an efficient use of the available energy from the array. Both the clamped and direct coupled systems performed essentially the same. The lack of charge regulation did not appear to affect the system ability to meet the load. Although not available in the current version of WATSUN-PV a tabulation of gassing current could show that the direct coupled system generates more battery gassing. Hence this approach is not favoured from an operational point of view.

A similar set of results were obtained by reducing the array size and increasing the number of batteries. The margin of reliability of the system, i.e. the minimum remaining obtainable charge in the battery, was strongly dependent on the array size.

The main conclusion that can be extracted from this part of the work is that no major differences in system performance were observed due to the control strategy adopted. Therefore, once the type of battery and array are selected, the control strategy should probably be chosen simply on the basis of capital cost or ease of implementation.

The enhanced battery model is temperature sensitive and based on I-V characteristics. It describes current-voltage behaviour rather than electrochemical behaviour. In its present format it accepts battery parameters in the form of voltage vs time and gassing vs voltage data. A complete default data set is provided for a typical lead acid battery so that the user can perform simulations without any battery data other than capacity. The user can also modify the input curves point by point using battery specific data.

Other battery types such as nickel-cadmium can be incorporated into the model. Except for different parameters, the non-gassing portion of the battery performance curves are similar to that of lead acid batteries. A model for the gassing regime of NiCd's will be developed in future phases of the program.

Battery self-discharge and self-heating and other minor effects were not modeled since they effects may not be significant in the applications discussed here.

Long term battery aging effects in a PV system are important because knowledge of the expected battery life under a set of operating conditions allows their replacement before failures occur. Incorporation of a battery aging model into a PV system simulation provides the designer with the tools to determine the effect of component sizing on battery discharge characteristics and consequently battery life.

The aging model developed in this project tracks the aging but does not modify the characteristics of the battery with life. This passive approach is justified because the greatest effect of

age is upon capacity. At the end of an annual simulation the user gets a report on the reduction of life suffered by the battery, the life expectancy under the same conditions and the volume of electrolyte lost to gassing.

In a PV-diesel hybrid system, in a typical northern Canadian site, the diesel generator operates mainly during the winter months to recharge the battery and power the load. This is followed by a few days in which the batteries supply the load. During the summer, the PV array and the batteries handle most of the energy requirements of the system. The generator is on a few hours a month, for maintenance procedures.

In the model implemented here the diesel generator was characterized by its capacity and the criterion for turning it on based on the status of the rest of the hybrid system. The fuel consumed is dependent on the altitude, temperature and type. Fuel efficiency curves were fitted to the cubic spline routines of WATSUN-PV and then derated for altitude and temperature.

The diesel generator always starts and stops on the hour. When it is called during the hour, the simulation is repeated. This simplification provided a form of hysteresis needed to prevent the generator from cycling on and off frequently.

The PV-diesel and battery aging models have been implemented in version 3.0 of WATSUN-PV. Systems simulations will be done by the Watsun group once the program has been fully debugged. It is intended that two remote stand alone systems with the same array but different annual energy distributions will be simulated. The results will be available to users and designers to carry out long term economic analyses. This will allow the examination of the sensitivity of the overall system costs to the correct battery and array sizings.

Several tasks remain to be carried out to make WATSUN-PV an useful program for the assessment of the design and the feasibility of PV-hybrid systems for use in remote northern Canadian locations.

In order for WATSUN-PV to be adopted by a broad spectrum of users, it should be as user friendly as possible. The implementation of user interfaces and the programming and debugging of user code is more easily done in Pascal than in Fortran currently used by WATSUN-PV. The more modular nature of Pascal facilitates the integration of code from multiple contributors.

The battery continues to be the most difficult component to model accurately due to its complex time dependence. It is recommended that high accuracy cell tests be performed with very well controlled current or voltage and temperature parameters to provide cycle repeatability. The results of these tests can be used to refine the mathematical model structure and improve the default battery parameters. Long term battery performance data are also required to quantify the aging model implemented here.

Finally, another version of the PV-diesel model should follow once the current model has been exercised by various interested parties and improvements and simplifications have been suggested

The seemingly very different tasks carried out in the present work have contributed significantly to the enhancement of WATSUN- PV and its use as an effective simulation tool for low power PV systems for the Canadian north. Further improvements to the program should be realized by a combination of the work that remains to be done and the experience gathered by third parties in the actual application of the software to real systems

## RÉSUMÉ

En collaboration avec le Groupe Watsun de l'University of Waterloo et de TdS Dixon Inc., ORTECH International a étendu et optimisé les ressources du logiciel WATSUN-PV. Ce programme peut simuler et évaluer les performances des systèmes PV basse puissance autonomes à batterie d'accumulateurs.

On a étudié les effets des différentes techniques de commande, de l'addition d'une génératrice Diesel et de la durée de vie des batteries sur les performances de système, et des modèles ont ainsi été élaborés en vue de leur intégration à ce qui est devenu la version 3.0 de WATSUN-PV.

Les sites éloignés du Nord canadien se prêtent bien à l'application générale des systèmes hybrides PV-Diesel. Les questions d'investissement initial et de fiabilité n'ont toutefois pas encore été totalement résolues. Les travaux décrits dans le rapport contribuent à une meilleure compréhension de l'interaction entre les différents éléments des systèmes hybrides, et ils fournissent un outil d'évaluation des performances des systèmes dans leur ensemble.

De nouveaux modèles de réseau PV et de batterie ont été élaborés dans le but d'appuyer l'application et la comparaison de cinq différentes techniques de commande et de simplifier l'utilisation de WATSUN-PV. Le nouveau modèle de réseau prédit les conditions horaires de courant et de tension (modèle I-V) en fonction de la température et du rayonnement solaire. Il admet aussi les paramètres de module qui sont disponibles des fabricants. Les techniques de commande de système qui ont été étudiées étaient les suivantes :

- poursuite de la puissance maximale du réseau avec tension de limitation de la batterie
- poursuite de la puissance maximale du réseau avec charge d'entretien de la batterie
- calage de la tension de réseau avec tension de limitation de la batterie
- calage de la tension du réseau avec charge d'entretien de la batterie
- couplage direct entre le réseau et la batterie

La façon la plus simple de comparer les diverses techniques de commande aurait consisté à les simuler sur cinq systèmes dans des conditions identiques de taille des éléments, de courant de charge et de données météorologiques, puis à comparer leurs performances. Dans la pratique, le choix d'une technique plutôt que d'une autre repose toutefois sur des critères économiques. On a donc effectué la comparaison en changeant la taille de chacun des systèmes de manière à obtenir les mêmes performances du point de vue de la fiabilité et de la charge. Toute comparaison entre les systèmes se fondera sur la taille relative des éléments et sur les économies ou les coûts correspondants.

Le processus itératif est plus laborieux, mais les résultats peuvent être utilisés directement dans une analyse économique.

La comparaison des cinq techniqes a été effectuée pour un

site éloigné (Inuvik, T.-N.-O.). Le système de poursuite du point de puissance maximale nécessitait moins d'accumulateurs. Le chargeur d'entretien ne faisant pas une utilisation efficiente de l'énergie fournie par le réseau. Les systèmes à calage et à couplage direct se comportaient essentiellement de la même façon. L'absence de régulation de charge n'a pas semblé influer sur l'aptitude du système à supporter la charge. Bien que non disponsible dans la version actuelle de WATSUN-PV, un tableau des courants de dégagement gazeux pourrait montrer que le système à couplage direct permet un dégagement plus intense, ce qui n'est pas souhaitable du point de vue de l'exploitation.

La réduction de la taille du réseau et l'augmentation du nombre de batteries ont donné des résultats semblables. La marge de fiabilité du système, soit la charge résiduelle minimale de la batterie, était fortement liée à la taille du réseau.

La principale conclusion que l'on puisse tirer de cette partie des travaux est qu'aucune différence majeure de performances des systèmes n'était liée à la technique de commande adoptée. Le choix d'une technique particulière demeure une décision économique, une fois que l'on a déterminé le type de batterie et de réseau à employer.

Le modèle de batterie amélioré est lié à la température et repose sur les caractéristiques I-V. Il décrit les caractéristiques courant-tension, plutôt que les caractéristiques électrochimiques. Sous sa forme actuelle, it admet les paramètres des batteries sous forme de tension en fonction du temps et de dégagement gazeux en fonction de la tension. Une fiche complète de données implicites est donnée pour une batterie au plomb typique, afin de permettre à l'utilisateur d'effectuer des simulations sans données autres que la capacité. L'utilisateur peut modifier les courbes d'entrée point par point à l'aide de données propres aux batteries.

La décharge spontanée et l'auto-chauffage de la batterie, ainsi que d'autres effets mineurs, n'ont pas été incorporés au modèle, étant donné que leur rôle peut être négligeable dans les applications en cause.

Les effets du vieillissement à long terme des batteries dans un système PV ont leur importance, car ce n'est qu'en connaissant la durée de vie prévue d'une batterie dans un ensemble de conditions opérationnelles qu'il est possible d'effectuer un remplacement avant que ne se produisent des défaillances. L'intégration d'un modèle de vieillissement de batterie à un programme de simulation de système PV donne au concepteur les outils nécessaires pour déterminer l'incidence de la taille des éléments sur les caractéristiques de décharge d'une batterie, et donc sur la durée de vie de celle-ci.

Le modèle de vieillissement établi pour ce projet suit le vieillissement, mais ne modifie pas les caractéristiques de la batterie selon la période de la durée de vie. Cette passivité se justifie du fait que le plus grand effet du vieillissement se fait sentir sur la capacité. A la fin d'une simulation annuelle, l'utilisateur obtient un rapport de la réduction de durée de vie de la batterie, de la durée de vie prévue dans les mêmes conditions et du volume d'électrolyte perdu en dégagement gazeux.

Dans un système hybride PV-Diesel utilisé à un site typique du Nord canadien, la génératrice Diesel fonctionne principalement durant les mois d'hiver pour recharger la batterie et alimenter la charge. Suivent ensuite quelques jours pendant lesquels les batteries alimentent la charge. Durant l'été, le réseau PV et les batteries satisfont à la majeure partie des besoins du système. La génératrice ne fonctionne que quelques heures par mois à des fins de maintenance.

Dans le modèle dont il est question ici, la génératrice Diesel se caractérise par sa capacité et son déclenchement est lié à l'état du reste du système hybride. Le carburant consommé dépend de l'altitude, de la température et du type utilisé. Les courbes d'efficience d'utilisation du carburant ont été adaptées aux routines à fonction pistolet cubique de WATSUN-PV, puis soumises à un abaissement des valeurs tenant compte de l'altitude et de la température.

C'est toujours à l'heure juste que la génératrice Diesel se met en marche et s'arrête. La simulation se répète lorsqu'un appel se produit entre temps. Cette simplification fournit la forme d'hystérésis nécessaire pour empêcher la génératrice de suivre un cycle de fréquentes mises sous tension et hors tension.

Les modèles PV-génératrice Diesel et de vieillissement de batterie ont été intégrés à la version 3.0 de WATSUN-PV. Le groupe Watsun effectuera les simulations de système une fois que le programme aura été complètement débogué. On prévoit simuler deux systèmes autonomes éloignés utilisant le même réseau, mais fonctionnant selon différentes distributions annuelles d'énergie. Les résultats seront mis à la disposition des utilisateurs et des concepteurs en vue d'analyses économiques à long terme. Il sera ainsi possible d'examiner dans quelle mesure les coûts totaux de système dépendent du choix de la batterie appropriée et de la taille du réseau.

Plusieurs tâches demeurent encore pour faire de WATSUN-PV un programme utile d'évaluation de la conception et de la faisabilité des systèmes hybrides PV destinés aux sites éloignés dans le Nord canadien. Pour être adopté par un large éventail d'utilisateurs, WATSUN-PV doit être aussi convivial que possible. L'implantation des interfaces utilisateurs ainsi que la programmation et le débogage des codes d'utilisateur s'effectuent plus facilement en Pascal qu'en Fortran, soit le langage actuellement utilisé par WATSUN-PV. Le nature plus modulaire du Pascal facilite l'intégration des codes d'origines multiples.

En raison de ses liens complexes avec le temps, la batterie est toujours l'élément le plus difficile à modéliser adéquatement. Il est recommandé de soumettre les accumulateurs à des essais de haute précision en utilisant des paramètres très rigoureux de courant ou de tension ainsi que de température, de manière à assurer la répétabilité du cycle. Les résultats de ces essais peuvent servir à raffiner la structure du modèle mathématique et à améliorer les paramètres implicites des batteries. Des données sur les performances à long terme des batteries sont également nécessaires à la quantification du modèle de vieillissement dont il est question ici.

# 1. Introduction

This final report describes the work carried out by Ortech International and its sub-contractors on contract serial number 23283-7-6130/02-SS; "Enhancement and Application of PV Systems Simulation Package". The work dealt with the extension and optimization of the WATSUN-PV system simulation package initiated in the previous phase of this program [1]. The simulation software capabilities were extended to include the effect of different control strategies on system performance. At the same time, models were developed to account for the addition of a diesel generator and the effect of battery aging on overall system performance.

Non-conventional power systems are required in sites far from power grids or where fuel supply and transportation costs are high. Solar PV/diesel hybrid generation with battery back-up is one of the most attractive non-conventional energy sources for environmental and economic reasons.

Remote northern Canadian sites are a prime candidate for the widespread application of these systems if capital costs can be reduced while at the same time, system reliability and life are improved. The extreme climatic conditions in many remote Canadian sites pose unique problems. The combined effect of low temperatures, low insolation and difficult access impose a premium on the performance of the PV system components

At the present time, batteries are the best form of energy storage because of their availability and relatively low cost. However, batteries for remote PV systems must possess high charging efficiency, low self discharge, low maintenance and the ability to operate at various state of charge in a wide temperature range.

Additional system component data, design criteria and test procedures are needed by Canadian designers together with optimized simulation tools. Work in these areas has been carried out mostly by groups in Europe and the U.S. for applications that are not representative of northern Canadian sites [2-4].

For the last several years Ortech International, the Watsun Group and a few others have been supplying some of the missing data on PV and battery technologies [1,5]. A three pronged approach has been used to i) generate low temperature battery performance, ii) develop better battery and PV array models and iii) develop a full software package for the simulation of low power PV systems operating under extreme conditions.

In the present phase of the program, reported here, Ortech International continued the collaboration with the Watsun Group and TdS Dixon Inc. in the development of new models and the implementation of a new version of WATSUN-PV which incorporates various enhancements and makes it more useful and general.

## 2. Objectives

The general objective of this program is to continue building up expertise in the simulation of the performance of PV systems for use in the Canadian north. This expertise is expected to benefit users and designers of systems that must operate efficiently in remote applications.

The specific objectives of the present phase of the program were:

i) To determine the effect of different system control strategies on system performance and battery life;

ii) To develop and implement a PV-diesel model and a battery aging model for inclusion in WATSUN-PV for stand alone PV systems.

# 3. Model Development for Non-hybrid Control Strategies

WATSUN-PV 1.0 simulates the performance of a stand-alone PV system with the use of energy models. The load is specified as an hour by hour energy profile. This method makes the simulation of control strategies based on system current and voltage impossible.

The shortcomings of the existing models in WATSUN-PV 1.0 could have been circumvented by using manual methods and temporary undocumented modifications to the code. The approach adopted, however, was to replace the existing models by new ones based on current-voltage (I-V) characteristics for the battery and the PV array which are suitable for the comparison of different control strategies.

In the previous phase of this program, battery evaluation supported the development of a temperature sensitive I-V based battery model within the WATSUN-PV energy simulation. This was then interfaced to the array in a relatively simply manner. The power from the array was considered constant over the period of an hour. The current available to the battery was determined on the basis of the battery voltage as in equation (1)

$$I_{array} = P_{array} / V_{battery} \qquad (1)$$

This simplification assumes that the array operates at a constant power regardless of voltage. This is only true in the case of a maximum power point tracked system.

A similar interface was constructed between the load and the battery. The approximation was reasonable since most loads can be considered constant power devices within certain limits.

In the present project, a decision was made to model the following system control strategies:

| | |
|---|---|
| 1) MPPT, Vmax | A maximum power point tracked array with battery charging controlled by limiting the battery voltage. |
| 2) MPPT, Trickle | A maximum power point tracked array with battery charging limited to a small current, after a preset battery voltage is reached. |
| 3) Clamp, Vmax | A system with the array voltage clamped to the battery; battery charging controlled by limiting the battery voltage. |
| 4) Clamp, Trickle | A system with the array voltage clamped to the battery; battery charging limited to a small current after a preset battery voltage is reached. |
| 5) Direct Coupled | Direct connection from the battery to the array; no charge control. This can be considered a clamped system. |

Simulation of the latter four strategies was impossible given the existing models in WATSUN-PV.

Another serious limitation of the existing I-V model of the battery was the lack of proper parameterization. There was no simple manner in which the user could take battery test data, and specify the characteristics of the battery to the model.

Consequently, new array and battery models were proposed and developed as described below.

## 3.1 Enhancement of PV Array Model

The new array (cell) model has the following characteristics:

a) It predicts hour-by-hour current and voltage conditions at the array as a function of temperature and solar radiation available.

b) It accepts specification parameters readily available from module (cell) manufacturers.

c) It is computationally efficient (unlike other module (cell) models such as TRNSYS.

The output of PV modules is generally described by an I-V curve which varies with temperature T and radiation Q such that I = I(V,Q,T). The array model developed herein follows a similar approach to that of Singer et. al. [6]

The classical equation describing the I-V curve of a single solar cell is

$$I = I_0\left(\exp\left[\frac{q}{AKT}(V+IR)\right]-1\right) + I_L \qquad (2)$$

Where $I_0$ = diode saturation current; $I_L$ = photocurrent
R = series resistance; T = absolute temperature
q = charge of electron; A = constant

The dependence on V and T are evident, $I_L$ and R are functions of Q. Equation (2) describes the I-V curve closely, but the parameters A, $I_0$ and $I_L$ are not easily measurable.

Equation (2) is shown in Figure 1.

On the other hand, parameters that are easily measurable are:

1) Open Circuit Voltage ($V_{OC}$)
2) Short Circuit Current ($I_{SC}$)
3) MPP Voltage ($V_{MP}$)
4) MPP Current ($I_{MP}$)

Singer et.al. [6] have developed a simplified form of equation. (2) with the constraint that the new curve passes through $V_{OC}$, $I_{SC}$, and the maximum power point (MPP). Two key simplifications are:

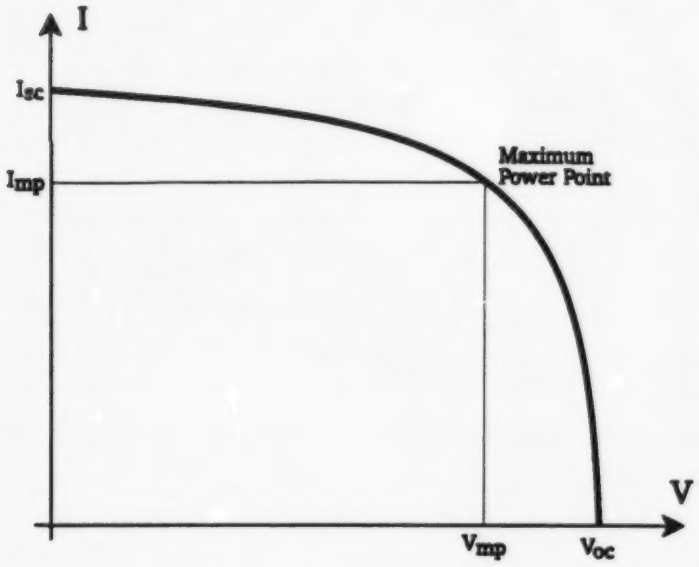


Figure 1 - Array I-V Curve

(a) $I_L \cong I_{SC}$

(b) the ratio $I_0 / I_{SC} = 10^{-9}$.

These simplifications are valid for silicon solar cells operating at approximately 25°C and 1000 W/m$^2$. Equation (2) takes the form:

$$I = I_{SC}\left[1 - 10^{-9}\exp\frac{20.7}{V_{OC}}(V + IR)\right] \qquad (3)$$

The quality of the fit to the actual I-V curve provided by equation (3) is illustrated in Figure 2. The actual I-V curve for a solar cell is plotted against that predicted by equation. (3).

The dependence of the cell I-V curve (represented by equation. (3)) on Q and T lies in the dependence of $V_{OC}$, $I_{SC}$, and R upon Q and T. Typical experimental data has shown that the dependence of the $V_{OC}$ and $I_{SC}$, on Q and T may be approximated by:

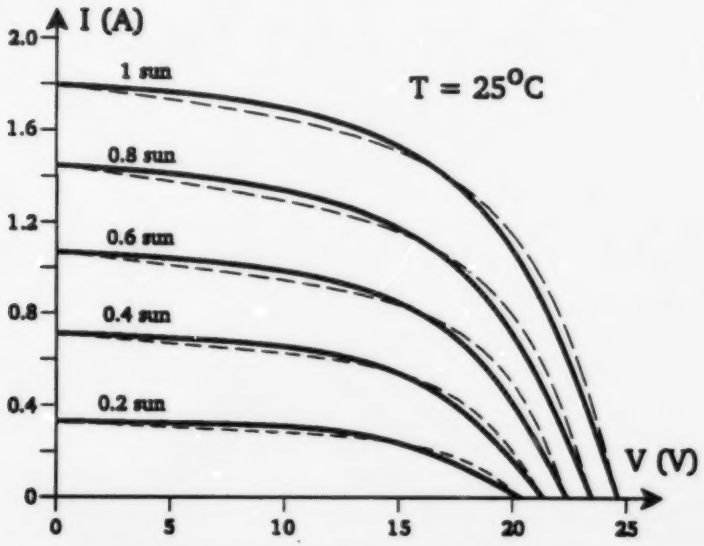


Figure 2 - Quality of Fit of Array I-V Curve
Solid curves are actual I-V curves for silicon solar cells.

$$I_{SC}(Q,T) = I_{SC}(ref)\ \frac{Q}{Q_{ref}}\ (1+\alpha(T-T_{ref})) \qquad (4)$$

$$V_{OC}(Q,T) = V_{OC}(ref)(1-\gamma(T-T_{ref}))\ \ln\left(e+\beta\left(\frac{Q}{Q_{ref}}-1\right)\right) \qquad (5)$$

Where: $V_{OC}$(ref) = open circuit voltage at Qref, Tref
$I_{SC}$(ref) = short circuit current at Qref, Tref
$Q_{REF}$ = reference radiation intensity
$T_{REF}$ = reference cell temperature

and typical values for a, B, and Y are:

$$\alpha = 0.0025 \quad 1/°C$$

$$\beta = 0.5$$

$$\gamma = 0.00288 \quad V/°C$$

In order to obtain a value for the series resistance R, at a given Q and T condition, a key assumption is made: the shape of the I-V curve does not change. This allows us to make the following approximations to locate the maximum power point at any radiation and temperature condition:

$$V_M(Q,T) = \frac{I_M(ref)\ V_m(ref)}{I_M(Q,T)} \left[\frac{I_{SC}(Q,T)\ V_{OC}(Q,T)}{I_{SC}(ref)\ V_{OC}(ref)}\right] \quad (6)$$

$$I_M(Q,T) = I_{SC}(Q,T)\ \frac{I_M(ref)}{I_{SC}(ref)} \quad (7)$$

where: $V_M(ref)$ = MPP voltage at $Q_{REF}$, $T_{REF}$
$I_M(ref)$ = MPP current at $Q_{REF}$, $T_{REF}$

Equation. (3) can be solved for R(Q,T) in terms $V_{OC}(Q,T)$, $I_{SC}(Q,T)$ and $I_M(Q,T)$:

$$R(Q,T) = \frac{V_{OC}(Q,T)}{20.7 I_M(Q,T)}\ \ln\left[10^{9}\left(1-\frac{I_M(Q,T)}{I_{SC}(Q,T)}\right)\right] - \frac{V_M(Q,T)}{I_M(Q,T)} \quad (8)$$

The procedure for determining the I-V curve for any temperature, and radiation condition begins with the input parameters $T_{REF}$, $Q_{REF}$, $V_{OC}(ref)$, $I_{SC}(ref)$, $V_M(ref)$, and $I_M(ref)$, defined above.

Equations (5) and (6) are used to obtain values for $I_{SC}(Q,T)$ and $V_{OC}(Q,T)$. Next, equations (6) and (7) are used to obtain values for $I_M(Q,T)$ and $V_M(Q,T)$. The series resistance R(Q,T) is now determined with equation (8). Finally we can solve equation (3) for cell current I, given cell voltage V:

$$I = I_{SC}(Q,T)\left[1 - 10^{-9}\exp\frac{20.7}{V_{OC}(Q,T)}(V + IR(Q,T))\right] \quad (9)$$

Equation (9) describes the I-V curve of a single cell but can be extended to a that of a module (or array of modules) by substituting the measured parameters of a module (or array). Singer et.al. [6] provide justification for this substitution.

If a maximum power point tracker is being used, then the current, voltage and hence output power of the array is completely determined by equations (6) and (7) above. It is not necessary to solve further. The simulation computes this power and then applies the efficiency factor specified for the MPP tracker to determine power to the battery. Equation (1) then interfaces the MPP tracker to the battery.

In the event that a direct coupled system or clamped system is being used the model uses the complete I-V curve specified by equation (9).

In either case, once an array current is determined this is applied to the battery. The battery model (section 3.2) then determines a new voltage, which in turn is used to determine a new array current. This process continues until the voltage converges.

At this point the control algorithms based upon voltage may be invoked depending on the conditions present and type of control specified. Details of these controls are provided in sections 3.2 and 3.3.

## 3.2 Enhancement of Battery Model

The new battery model has the following characteristics:

a) The model is temperature sensitive and current-voltage (I-V) based (as opposed to simply power based).

b) It accepts battery characteristics specifications in the form of voltage vs time and gas ($H_2$ and $O_2$) production vs voltage data directly.

c) A complete default data set is provided for a typical lead-acid battery to allow the user to perform simulations without any battery data other than capacity. The input curves can be modified point by point as data for a specific battery is used.

d) The model is general enough to be adaptable to Nickel-Cadmium (NiCd) and other types of batteries.

e) The model can easily provide both voltage as a function of current and current as a function of voltage. Previous models provided only voltage as a function of current and the inverse function had to be determined iteratively. This was a problem for any voltage limiting charge strategy.

Batteries are complex electrochemical systems. Models for predicting the current-voltage behaviour analytically, from first principles, are quite involved and have met with limited success. For this reason, the model developed for WATSUN-PV is phenomenological in nature. It is based upon a set of observations of current-voltage behaviour, rather than electrochemical behaviour. A similar approach has been followed for the battery model employed in TRNSYS [7] as discussed by Hyman et.al. [8]. The two models differ only in the input data provided by the user. In TRNSYS the user inputs parameters for an equation which is a "curve fit" to the batteries I-V curve. In WATSUN-PV the user provides actual data of voltage vs time.

### 3.2.1 Overview

A battery is a temperature dependent nonlinear device with a response based on its long, medium, and short term history. In contrast, all the other components of a PV system have relatively well defined response curves, depending only on instantaneous external factors.

Batteries have traditionally been modeled as a combination of several ideal components, such as an internal voltage and an internal impedance. These components would both vary with temperature and state of charge, so that the current-voltage characteristic could be determined for the existing conditions.

A further complication is the modeling of battery gassing. As a battery approaches full charge, an increasing proportion of any charging current will be used to produce hydrogen

gas, rather than to charge the battery. To include this effect in the model, a second current path is needed, with a gassing voltage and a gassing resistance. A full model of the battery then resembles Figure 3.

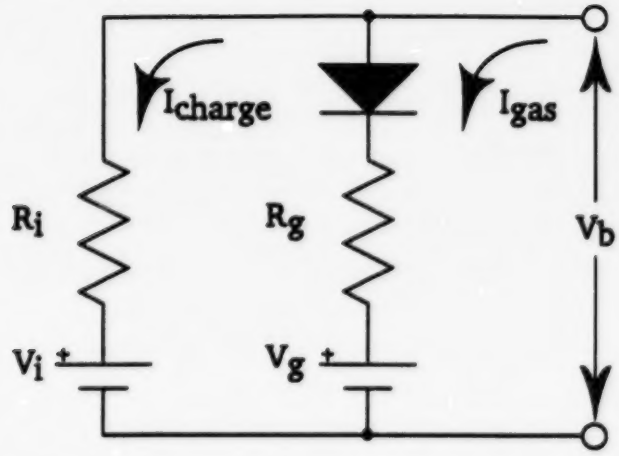


Figure 3 - Battery Model

$V_i$ and $R_i$, the internal voltage and resistance, vary with both temperature and state of charge. $V_g$ is the voltage above which gassing occurs at a given temperaturee. A diode is included in the gassing path of the circuit, because gassing does not occur until the battery voltage exceeds the gassing voltage. $R_g$ is the gassing resistance, which will start at a fairly large value and fall off to nearly zero as the battery becomes fully charged. When $R_g$ is near zero, $I_{gas}$ increases until it accounts for all of the battery current ($I_{charge}$ approaches zero).

While this circuit does provide a reasonable ideal model for the battery, nearly all of its components vary with the temperature and state of charge.

Clearly, what is required is a model which outputs battery voltage given the temperature, current, and preceding state of charge. This amounts to a relatively large curve fitting problem, where temperature, current, and state of charge are independent variables and voltage is the dependent variable. The temperature, current, and voltage are all externally measurable quantities while state of charge can be derived from a history of current into and out of the battery. Therefore, the whole curve fitting scheme can be developed from a series of charge and discharge curves supplied by the user, along with a curve of gassing current versus the difference between battery voltage and gassing voltage.

A fairly extensive laboratory characterization of batteries was carried out in Phase II of this program to support the modeling activities [1].

Ortech characterized 10 different types of batteries from different suppliers; 7 were lead acid and 3 were NiCd batteries intended for PV or remote power applications as recommended by the manufacturers.

The effect of low temperature (down to -40°C) and charge discharge rates on battery performance was determined. The experimental results were not very reproducible using industry standard test equipment. The batteries were strongly influenced by any irregularities in the test procedure such as over-charging or delays due to scheduling. Since in field applications similarly unpredictable conditions could be expected, these results could have been a demonstration of the unpredictability of actual battery performance.

Detailed high accuracy measurements were made on a lead acid and NiCd battery. Single cells were tested to prevent masking of the results by the potentially unsynchronized responses of various cells. The cells were sealed to enable the collection of the gas generated by gas-flow measuring apparatus.

The onset and degree of gassing was dependent upon cell voltage. The lead acid battery exhibited gassing which was independent of the charging rate. In the NiCd battery, the gassing rate behaviour was more complicated. In both cases, gassing at lower temperatures was suppressed, specially for the lead acid battery.

The charge-discharge cycles were repeated until a degree of cycle reproducibility was achieved. By using the voltage vs. gassing curve, the actual state of charge was known at all times (assuming gassing was the only source of coulombic loss). The high accuracy measurements provided information on cell voltage as a function of state of charge rather than time, for both charging and discharging at a specified current level and temperature [1]. Similar tests were performed during this phase of the program but at a reduced level of effort.

In the new battery model, the user can specify up to five charge and five discharge curves, of voltage versus time. The program then transforms these curves into voltage versus state of charge, using a process outlined in sections 3.2.2 and 3.2.3. Then it determines equations for the dependence of the V-Q line on both current and temperature. These equations are calculated at the beginning of the simulation, to reduce the amount of calculation that must be repeated each hour.

For a given hour, the following steps are carried out:

1. The V-Q line is adjusted for battery temperature.
2. The battery current from the previous period is used as an initial guess.
3. The V-Q line is adjusted for current.
4. The existing state of charge is used to determine the battery voltage.
5. This voltage is used to calculate array, load, and regulator currents.
6. A new value for battery current is calculated. If it is significantly different from the previously used value, the program returns to step 3. Iteration continues until the program converges on a value for current.

7. The calculated battery current is used to charge or discharge the battery for the period.

8. Using the new state of charge, and steps 3-6, a new value of battery current is calculated for the end of the period.

9. If the current has changed significantly, the hour is split in two, and steps 2-8 are carried out for each half hour.

10. The current determined at the end of the second half hour is compared with the previously determined current at the end of the hour. If the two are significantly different, the hour must be split again and steps 2-8 carried out for each quarter hour. The process of splitting the hour continues until convergence is reached.

Fortunately, battery current is usually quite stable in a given hour, so steps 9 and 10 are rarely carried out.

A great deal of work has gone into the solution process in the battery model. Once the answers produced were reasonable, the code had to be extensively refined to bring run time down to an acceptable level. Users with relatively slow computers will still find that a one year simulation runs in about half an hour. However, future versions of WATSUN-PV may be able to reduce this running time.

The battery model is intended to be general enough to represent both lead-acid and NiCd batteries adequately given appropriate parameters. For the most part, the charge and discharge curves provided by the user will describe a Ni-Cd battery just as well as a Lead-Acid battery, except for the gassing regime. The modeling of gassing may be different for Ni-Cd batteries: a second order function of charge rate as well as voltage may be required. Until this question is resolved, Ni-Cd batteries will be modeled as though they were Lead-Acid.

No attempt has been made to model either self-discharge or self-heating of batteries. Self-discharge is the tendency of a battery to lose charge slowly when no current is applied to it. This effect is probably present at all times, and should be modeled as a self-discharge current subtracted from the battery current. Self-heating is probably too small an effect to include in a model of this type. Batteries do tend to warm themselves up when a large current is applied, but in most northern applications where temperature is a concern, the number of batteries is so large that currents are very low.

There are also some medium and long term effects in batteries. Ni-Cd batteries in particular experience a phenomenon called "memory", in which repeated shallow discharge cycles cause the battery to lose its ability to deep discharge. This highly complex effect may not be worthwhile modeling in WATSUN-PV, particularly since it is reportedly not present in the newer Ni-Cd batteries using pocket plate technology.

A number of minor effects are unlikely to be included in future versions of WATSUN-PV. There are small nonlinear effects at very low currents. The model used in WATSUN-PV treats the three charge currents and three discharge currents as 6 points on one curve, so the function is smooth as it crosses between charge to discharge. The addition of self-discharge may account for the nonlinear effects near zero current, but in any case these effects are probably negligible except for very large, tightly controlled systems.

Stratification effects and unequal cell performance within a battery are ignored. The charge and discharge curves specified by the user are intended to be averages.

Transient effects within the battery, due to changes in current, have also been ignored. In most cases the time constants involved are in milliseconds, so their impact on an hourly simulation would not justify the computational effort required to simulate them.

Long term battery aging effects are described in Chapter 6..

### 3.2.2 Battery Discharge

In the input data for the batteries, the user specifies up to five different discharge curves for one cell of the battery, using up to three different temperatures and three different currents. If a full set of curves is supplied, they will be arranged as in Table 1.

Table 1

| Curve | Temperature | Current |
|---|---|---|
| 1 | $T_1$ | $I_1$ |
| 2 | $T_1$ | $I_2$ |
| 3 | $T_1$ | $I_3$ |
| 4 | $T_2$ | $I_2$ |
| 5 | $T_3$ | $I_2$ |

where $T_1 > T_2 > T_3$ and $I_1 > I_2 > I_3$

Note that these currents are all specified as positive values.

A typical set of points for a discharge curve for one cell of a 6-cell, 10 Ah lead-acid battery might be as shown in Table 2.

Table 2

| Point | Time(hours) | Voltage(V) |
|---|---|---|
| 1 | 0.00 | 2.030 |
| 2 | 11.50 | 1.980 |
| 3 | 16.00 | 1.940 |
| 4 | 19.00 | 1.860 |
| 5 | 19.98 | 1.751 |

where: T = 20°C and I = 0.5 A

The discharge curve is assumed to consist of a linear section beginning at time 0 and running through the first two points followed by a nonlinear section running through the remaining three points and terminating at the cutoff voltage specified. If this is a 6-cell battery with a cutoff at 10.5V, then the cutoff for one cell would be 1.75V, which would occur very shortly after the 5th point specified.

The model assumes that a battery does not experience losses during discharge; all inefficiencies are taken into account during the charge cycle. Therefore, it is a simple matter to change a voltage versus time curve into a voltage versus charge curve by multiplying the time by the current. If we then solve for the point where V = 1.75 volt, we can determine the discharge capacity at the present conditions of temperature and current. In this case, the capacity is calculated as 9.99 A-hr.

A state of charge for these conditions is now defined, with a value of 1 at the beginning of the discharge cycle and a value of 0 at the cutoff voltage. A plot of voltage versus state of charge is shown in Figure 4.

The V-Q curve is now fully defined for T = 20°C, I = 0.5 A discharge. It has a linear section from SOC = 1 to SOC = 0.4246, with a slope of 0.0869 and an intercept of 1.9431. This is followed by a nonlinear section beginning at SOC = 0.4246, V = 1.98 and ending at SOC = 0, V = 1.75. In the simulation process, this nonlinear section is approximated using a cubic spline curve fit.

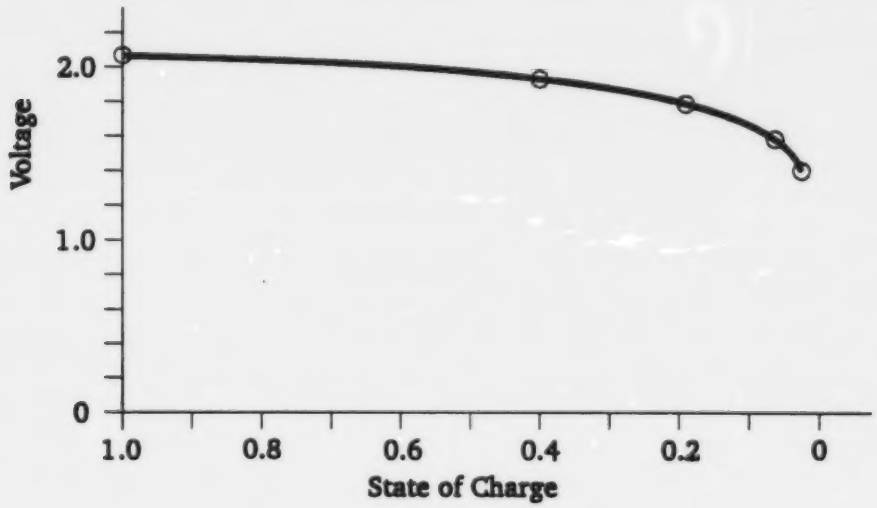


Figure 4 - Battery Discharge Curve

### 3.2.3 Battery Charge

Charging is a slightly more complicated process than discharging, because losses due to gassing are introduced. The input data again includes up to five different curves for a single cell of the battery, using up to three different temperatures and three different currents. If a full set of curves is supplied, the arrangement is exactly the same as in Table 1.

A typical set of points for a charge curve for one cell of a 6-cell, 10 Ah lead-acid battery might be as in Table 3.

Table 3

| Point | Time(hours) | Voltage(V) |
|---|---|---|
| 1 | 0.00 | 2.100 |
| 2 | 14.00 | 2.300 |
| 3 | 15.50 | 2.375 |
| 4 | 16.50 | 2.620 |
| 5 | 18.00 | 2.650 |

where: T = 20°C and I = 0.5 A

The charge curve is assumed to consist of a linear section running through the first two points followed by a nonlinear section running through the remaining three points and terminating when the battery is fully gassing.

The gassing of the battery is described using a set of five points on the curve of gassing current versus battery voltage minus gassing voltage. This curve can be derived from measurements of the hydrogen gas produced by the cell as its voltage is increased above gassing voltage. Gassing curves for a standard lead-acid cell are easily available in the published literature. A curve for this 10 A-hr battery is shown in Figure 5.

This curve can be used to determine the termination point for the charge curve, i.e. the point where the battery is fully gassing. The current for this charge curve is 0.5 A, which corresponds to a voltage difference of 0.4V. A cubic spline function is used for this interpolation in the program. If the second point on the charge curve, (14 hours, 2.3V), is taken as the point where gassing starts, the termination point will therefore be at 2.3 + 0.4 = 2.7 V.

The program extrapolates using the three points in the nonlinear region, to determine how long the battery would take to reach 2.7 V. Then it integrates the value of battery current minus gassing current over the entire charge period to determine the number of ampere-hours that have gone into the battery. SOC is assumed to be 1 at V = 2.7 V, and the battery capacity is still 9.99 A-hr, as calculated for the discharge curve under the same conditions. It is therefore possible to work backwards to determine SOC at each point on the charge curve. A plot of voltage versus state of charge is shown in Figure 6. The gassing current is shown on the same plot.

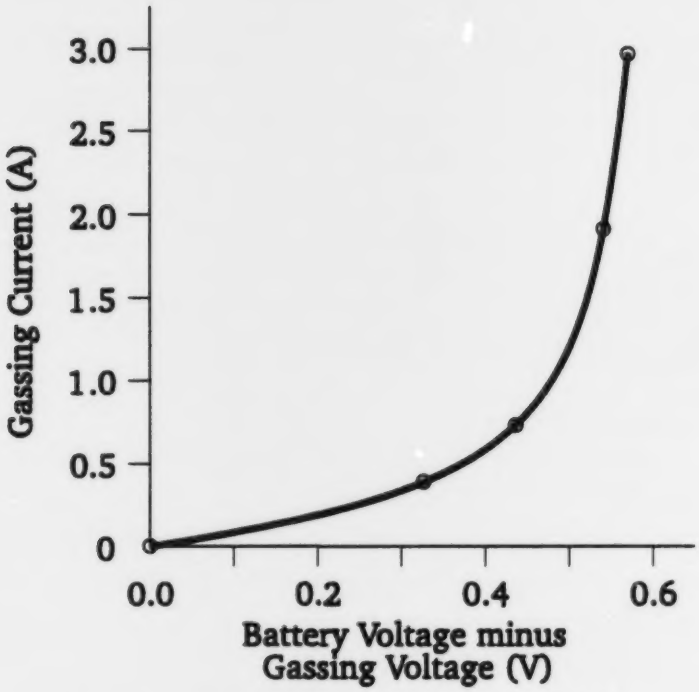


Figure 5 - Battery Voltage Minus Gassing Voltage

The V-Q curve is now fully defined for T = 20°C, I = 0.5 A charge. It has a linear section from SOC = 0 to SOC = 0.7725, with a slope of 0.2855 and an intercept of 2.0794. This is followed by a nonlinear section beginning at SOC = 0.7725, V = 2.30 and ending at SOC =1, V = 2.70. In the simulation process, the nonlinear section is approximated by a cubic spline. When the battery is operating above 2.3 V per cell, the gassing current will be calculated using another cubic spline curve fit.

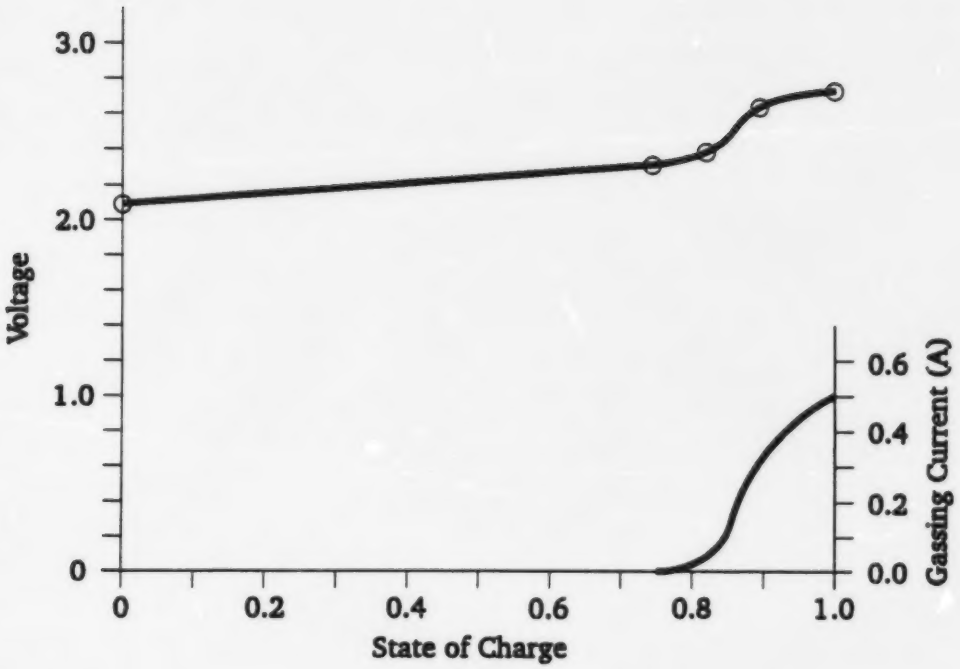


Figure 6 - Battery Charge Curve

### 3.2.4 Temperature and Current Dependence

Sections 3.2.2 and 3.2.3 outline how the program analyses each charge and discharge curve, to arrive at a V vs Q function. If the user wishes to include the temperature dependence of the battery in the simulation, at least 2 charge and discharge curves must be supplied, at different temperatures.

At the beginning of each hour, the following temperature dependencies are calculated:

(a) maximum battery voltage

(b) charging voltage at which gassing begins and the V vs Q curve ceases to be linear

(c) available battery capacity

(d) slope of the linear section of the V vs Q curve

(e) V-axis intercept of the linear section of the V vs Q curve

(f) voltages in the nonlinear charge region beyond point (b) above

(g) voltage at which linear portion of the V vs Q curve during discharge ends

(h) voltages in the nonlinear discharge region

The V-Q function in WATSUN-PV also varies with current. It is important that the input data include charge and discharge curves at more than one current in order for this solution process to perform properly. With only one charge and discharge curve, the program will usually fail to model correctly.

After completing the temperature dependent adjustments, current dependencies are accounted for on most of the same parameters listed for temperature.

The mathematical details of these temperature and current adjustments are complicated and are provided in the WATSUN-PV user's manual [9] under the sections defining the battery model.

### 3.2.5 Convergence Procedures

Each hour, the battery voltage is calculated as outlined in sections 3.2.2 through 3.2.4 as a function of battery temperature and estimated battery current. The battery temperature is a known parameter for the hour. The battery current, however, is not a known and is initially estimated as the value calculated for the previous simulation hour. This battery voltage is then used to recalculate the currents in the rest of the PV system: array current; load current; regulator current. A new estimate for battery current can then be calculated using

$$I_B = I_A - I_R - I_L \qquad (10)$$

where: $I_B$ = battery current
$I_A$ = array current
$I_R$ = regulator current
$I_L$ = load current

The difference between this new value for battery current and the original value corresponds to how far the battery current is from the correct solution. The original and the re-estimated battery currents are used to estimate a new battery current and hence voltage and then yet another estimate for the battery current. Normally, the secant method is employed to select each subsequent estimate for the battery current. The iterative cycle is repeated until either satisfactory numerical convergence is achieved or until it is clear that proper convergence will not occur (ie: if the battery is operating above its maximum allowable voltage or if the estimates for the battery current begin to diverge). If convergence cannot be reached, the secant method is abandoned, and the system reverts to the bisection method. The bisection method is slower to converge, but is less prone to instability than the secant method.

### 3.2.6 State of Charge

One of the most difficult issues in developing a battery model is to determine the relationship between state of charge at one set of conditions and state of charge at another set of condi-

tions. If a battery is completely discharged at -10°C, it can be warmed up to 20°C, for example, giving off more energy. A lower discharge current can also enable more energy to be removed after the battery is apparently discharged.

In fact, there are two definitions for state of charge. Absolute state of charge is expressed in coulombs and is affected only by the net charge that is transferred to or from storage in the battery. The zero point for absolute state of charge is arbitrary. Changes in other conditions such as temperature do not affect the absolute state of charge, only its availability for transfer.

Relative or temperature adjusted state of charge is not measured in coulombs. Instead it is a dimensionless number between 0 and 1 where 0 represents the situation where no further discharge is possible and 1 represents the situation where no further charge is possible. Changing the battery temperature or charge or discharge current will immediately alter the temperature adjusted state of charge.

It is clear from the experimental data that a low temperature adjusted state of charge is strongly affected by changes in temperature (ie: a fully discharged battery at a low temperature will discharge further if it is warmed). It is not clear whether a high temperature adjusted state of charge (ie: 1) is affected by temperature. In the absence of evidence to the contrary, we have assumed that it is unaffected at the high end.

The calculations in sections 3.2.2 through 3.2.4 use for the most part temperature adjusted state of charge. This is derived, however, from an absolute state of charge integral which is computed for each time step using equation 10:

$$Q' = Q + (I_B - I_{GAS})\ \Delta T \qquad (11)$$

where: $Q'$ = new value for absolute state of charge
$Q$ = previous value for absolute state of charge
$I_B$ = battery current
$I_{GAS}$ = battery gassing current
$\Delta T$ = time step

### 3.2.7 Reduction of Time Step Size

WATSUN-PV is primarily an hour-by-hour simulation program. As such, it assumes that the currents in the system all remain constant during any one hour period. However, since systems may experience rapid changes in battery voltage that affect the currents (particularly near end of charge or discharge or if the batteries are small) this assumption is checked at the end of the hour.

If battery current has changed significantly, the hour is split into two halves and the calculations are carried out for the first and second half-hour. The battery current at the end of the second half-hour is compared to that previously obtained at the end of the full hour. If the difference is significant, the hour is split by another factor of two once again. This iterative cycle is limited to a time step of 1/32 hour, or approximately 2 minutes.

In practice, the process of splitting the hour is rarely required, because currents are generally quite stable over the period of one hour, especially if the batteries in the system are quite large. However, the process is available when it is required.

## 3.3 Addition of Several Control Modes

A wide variety of control strategies can be simulated in various combinations by WATSUN-PV:

a.) The array can be controlled by means of a maximum power point tracker (MPPT) or it can be clamped to the battery voltage.

b.) The end of battery charging can be limited to a maximum voltage, switched to a trickle charge after reaching a set voltage or simply coupled directly to the array without any end of charge protection. The third case does not exist within a MPPT.

c.) The end of charge regulation can use either series or shunt circuitry. The losses associated with this choice for the MPPT are usually built into its overall efficiency, so this choice is only considered explicitly for the clamped case.

With MPPT, the voltage of the array can vary independently of the battery voltage. This enables the controller to seek the array voltage which will obtain the highest power from the array under the given radiation conditions. A controller efficiency must be specified by the user. The power which can be supplied by the MPPT controller to the batteries or load is then equal to the available array power multiplied by the efficiency.

A MPPT system will include a mechanism to reduce its output to the battery near the end of charge either by limiting the voltage or by switching to a low trickle current.

For systems not using a MPPT, the array voltage is, except for end of charge regulation, clamped directly to the battery voltage. Except for direct coupled systems, end of charge will be regulated either by limiting the voltage or by switching to a low trickle current. Unlike MPPT systems, the end of charge regulation is modeled either as series or shunt circuitry and the associated inefficiencies explicitly characterized.

In simple systems, there may be no regulator at all. In this case the array is wired directly to the battery and their voltages are clamped at all times. The battery is unprotected against overcharging, and may experience a great deal of gassing if not sized precisely.

A series regulator consists of a switch, either electronic or mechanical, in series with the array. It controls current to the battery by switching the array on or off. There is no voltage drop associated with it, so the array voltage is equal to the battery voltage whenever the array is on. However, the switch draws a small current when the array is on, representing a loss to the system. The current loss associated with the relay or transistor, used as a switch, must be specified by the user.

A shunt regulator consists of a switch to shunt the current back to the array in order to control current to the battery. Since this switch is normally open, there is no current loss when the array is on. However, there is a diode in series with the array, to avoid short circuiting the battery when the shunt is operating. This means that the array will operate at a voltage equal to the sum of the battery voltage and the diode voltage. The voltage drop across the diode must be specified by the user if different from the default value of 0.6V.

# 4. Comparison of Non-hybrid Control Strategies

## 4.1 General Approach

The simplest means of comparing the non-hybrid control strategies would have been to simulate the five control strategies on five systems with identical component sizing, load requirements and meteorological conditions and then compare their performances. Performance improvements might include a greater proportion of the full load being met or a higher minimum state of charge and therefore greater margin of reliability.

However, the decision of whether to choose a more sophisticated control strategy over a simpler one is usually one of economics and it is difficult to put a direct monetary value on most performance improvements.

Instead of just reporting the relative performances of each control strategy in a sample system, we elected to translate the performance gains back into something that could more easily be given a monetary value. This was done by re-sizing each of the systems so that they all yielded the same level of performance in terms of reliability and load met. Any comparison between systems will then be based upon the relative component sizing and the corresponding cost savings or penalties. Although such an iterative process is more time consuming, the results could then be used directly in an economic analysis.

## 4.2 Results and Conclusions

### 4.2.1 Base Case

The five possible control approaches have been simulated in a simple sensitivity analysis. The objective of this analysis was to show the effect of the different methods of control on system performance.

A typical system configuration was chosen, as detailed in Table 4. Inuvik in the Northwestern Territories was selected for its greater than 100 day long nights. The reference system had a MPPT array control and maximum voltage charge control. By trial and error, an initial array and battery sizing was obtained, as shown on line 1 in Table 5 for each control strategy.

This system was 100% reliable as simulated; it always satisfied the load requirements. The minimum remaining obtainable charge in the battery was selected as a measure of the "margin of reliability". Initially this was found to be 366 Ah at -46°C. Based on a nominal capacity of 72 Ah (20h rate, 20°C) and approximately 100 batteries, the relative margin of reliability was 4.3%.

This margin of reliability was subsequently chosen as a target for the battery sizing when using the other four control strategies shown in Table 5. In this way, users could apply the results to perform economic analyses of specific installations and select the most cost efficient control strategy.

Because of the discrete size of the batteries, it was not possible to achieve identical margins in all the simulations. Values were matched as close as possible; a standard deviation is provided for the resulting range.

Three distinct observations can be made from the results shown in Table 5. The maximum power point tracked system requires less storage, probably because more energy is available from the array. In these systems the trickle charger does not appear to make as efficient use of the energy available from the array. Finally, the clamped and direct coupled system seem to perform essentially the same.

The latter only differ in charge regulation; the direct coupled is essentially a clamped configuration. The lack of charge regulation does not appear to affect the systems ability to meet the load, given a similar total battery capacity. Although not available in this version of WATSUN-PV, a tabulation of gassing current would show that the direct coupled system generates more battery gassing. Hence it is not favoured from an operational standpoint.

### 4.2.2 Reduced Array Size

The effect of different control strategies upon a system with minimal array size was investigated next. The array size of the reference system (MPPT, Vmax) was reduced from 216 Wp to 180 Wp (Table 6). The margin of reliability dropped to 72 Ah, or 0.85%. The battery size for each of the remaining control strategies was determined using the margin of reliability as a target. The removal of another module (18 W) would lead to the failure of the system to satisfy the load requirements all of the time.

The results show quite clearly that the MPPT system performs marginally better; there is little if any difference between the charge control strategies, and the direct coupled system performs equally as well as the MPPT system. This is likely a consequence of the module and battery voltages present. A mismatched directly coupled system would be expected to exhibit poorer performance than the MPPT system.

### 4.2.3 Undersized Array and Upsized Battery

Next, the array was reduced in size, by one module (Table 7). Consequently the reference system (MPPT, Vmax) did not satisfy the load requirements all of the time. To overcome this, the battery was up-sized, until the system yielded the same margin of reliability achieved in the base case analysis (Table 5). Batteries for each of the remaining systems were then sized to yield a similar margin of reliability.

Again, the results support the pattern observed in the previous simulations, that the MPPT requires less battery capacity than the clamped system. Additionally, it is quite clear from the results that the directly coupled system is operating as effectively as the MPPT system. Further discussion of the reasons for this behavior is presented in the next section.

Consider the results from the (MPPT, Vmax) system from Tables 5, 6 and 7, summarized in Table 8. The margin of reliability appears to be strongly dependent on the array size. On the other hand, the battery reliability is also very critical, as the system must operate during more than 100 days of darkness. It is therefore surprising that the array dependence is so strong.

It is clear from Tables 5 and 7 that there are no major differences in system performance due to the control strategy adopted. As mentioned above, the choice of strategy should be based primarily on capital cost and ease of implementation.

## Table 4 - System Specification

System Characteristics

| | | |
|---|---|---|
| **General** | | |
| Site | Inuvik N.W.T. | |
| Simulation Period | 1 year (1970 weather data) | |
| **Control** | | |
| Maximum Charge Voltage | 14.3 V | |
| Voltage Temp. Coef | 0.005 V/°C | |
| Trickle Charge Current | 100 mA | |
| Regulator Type | Series (0.15 A) | |
| **Modules/Array** | 18 watt | 72 watt |
| Slope | 75° | |
| Azimuth | south | |
| Ref Temperature | 20°C | |
| Ref MPP Voltage | 16.0 V | |
| Ref MPP Current | 1.125 A | (4.5 A) |
| Ref O/C Voltage | 19.0 V | |
| Ref S/C Current | 1.2 A | (6.0 A) |
| **Battery** | | |
| Type | Lead-Acid | |
| Battery Capacity | 72 Ah (20 h rate) | |
| Test Data (temps) | 20°C, -20°C, -40°C | |
| (currents) | 3.6 A, 1.06 A, 0.01 A | |
| **Load** | | |
| Type | Power specified | |
| LVD voltage | 11.7 V | |
| Daily Load | 400 Wh | |
| Description | 4 - 1 hour 100 Wh "spikes" One every 6 hours | |

Table 5 - Base Case

Module Size = 72 Wp
Battery Capacity (20 hr) = 72 Ah

| | No. of Modules | No. of Batteries |
|---|---|---|
| MPPT, Vmax | 3 | 100 |
| MPPT, Trickle | 3 | 102 |
| Clamp, Vmax | 3 | 103 |
| Clamp, Trickle | 3 | 105 |
| Direct Coupled | 3 | 103 |
| Minimum SOC | 366 | +/- 12 Ah |

Table 6 - Minimum Possible Array for Battery

Module Size = 18 Wp
Battery Capacity (20 hr) = 72 Ah

| | No. of Modules | No. of Batteries |
|---|---|---|
| MPPT, Vmax | 10 | 100 |
| MPPT, Trickle | 10 | 100 |
| Clamp, Vmax | 10 | 104 |
| Clamp, Trickle | 10 | 103 |
| Direct Coupled | 10 | 100 |
| Minimum SOC | 72 | +/- 15 Ah |

Table 7 - Undersized Array, Upsized Battery

Module Size = 18 Wp
Battery Capacity (20 hr) = 72 Ah

| | No. of Modules | No. of Batteries |
|---|---|---|
| MPPT, Vmax | 9 | 110 |
| MPPT, Trickle | 9 | 110 |
| Clamp, Vmax | 9 | 114 |
| Clamp, Trickle | 9 | 114 |
| Direct Coupled | 9 | 110 |
| Minimum SOC | 361 | +/- 16 Ah |

Table 8 - Summary of (MPPT, Vmax)

| Case | No. of 18 Wp Modules | No. of 72 Ah Batteries | Margin of Reliability |
|---|---|---|---|
| 1 | 12 | 100 | 366 +/-12 Ah |
| 2 | 10 | 100 | 72 +/-15 Ah |
| 4 | 9 | 100 | Failure |
| 4 | 9 | 110 | 361 +/-16 Ah |

### 4.2.4 Detailed Analysis of Results

A number of key system parameters were tracked for each of the simulations performed as part of this comparison. Figure 7 shows the energy flows represented by these parameters.

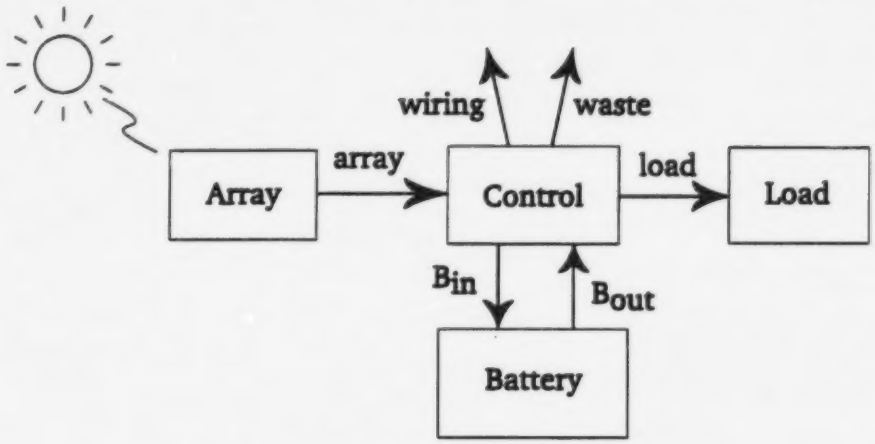


Figure 7 - PV-System Energy Flows

Briefly these flows represent:

| | |
|---|---|
| Array | - energy available from the array |
| Battery In | - energy used for battery charging |
| Battery Out | - energy extracted from the battery |
| Waste | - energy not used by the system |
| Wiring | - energy lost to voltage drops |
| Load | - energy delivered to the load |

These five parameters describe completely an energy balance upon the system:

Array + Battery Out = Battery In + Waste + Wiring + Load

The net flow of the battery represents energy lost to gassing and thermal losses. The simulation year begins and ends sometime in the summer so that the battery is fully charged at the beginning and end of the simulation.

For simplicity, the wiring resistance in these systems is set to zero, the only loss is the regulator voltage drop in the case of the clamped system.

Considering these parameters, further conclusions may be drawn from the detailed results of the 15 simulations of Tables 5, 6 and 7 given in Tables 9, 10 and 11.

In addition to the above parameters, the actual value of the reliability margins are given showing the variations in battery capacity caused by the range of values. The apparent flipping of the battery requirement between Table 9 and 10 for the clamped voltage systems is due to differences in the margins of reliability achieved.

The presence of the wiring loss in the clamped system explains quite reasonably the increased requirement for batteries in these systems. Although in the direct coupled system and clamped the amount of energy available from the array is the same, the presence of wiring losses has driven up the battery requirement.

In all cases the effect of the maximum power point tracker is clearly evident. Significantly more energy is collected. If, however, the balance of the system cannot use this energy effectively, the benefit is lost. A clear demonstration of this is the fact that the direct coupled system in Table 11 requires approximately the same battery capacity as do the MPPT systems. The questions arises; is the additional cost and reduction in operational reliability worth the small benefit of MPPT control?

## Table 9 - Base Case

Module Size = 18 Wp
Battery Capacity (20 hr) = 72 Ah

| | No. Modu | No. Batt | Array (MWh) | Bin (MWh) | Bout (MWh) | Waste (MWh) | Wiring (MWh) | SOCmin (Ah) |
|---|---|---|---|---|---|---|---|---|
| MPPT, Vmax | 12 | 100 | 0.238 | 0.135 | 0.119 | 0.077 | 0 | 366 |
| MPPT, Trickle | 12 | 102 | 0.238 | 0.135 | 0.119 | 0.077 | 0 | 373 |
| Clamp, Vmax | 12 | 103 | 0.213 | 0.135 | 0.120 | 0.044 | 0.08 | 343 |
| Clamp, Trickle | 12 | 105 | 0.220 | 0.130 | 0.100 | 0.050 | 0.08 | 376 |
| Direct Coupled | 12 | 103 | 0.221 | 0.134 | 0.119 | 0.060 | 0 | 374 |
| Minimum SOC | 366 | +/- 12 Ah | | | | | | |

## Table 10 - Minimum Possible Array for Battery

Module Size = 18 Wp
Battery Capacity (20 hr) = 72 Ah

| | No. Modu | No. Batt | Array (MWh) | Bin (MWh) | Bout (MWh) | Waste (MWh) | Wiring (MWh) | SOCmin (Ah) |
|---|---|---|---|---|---|---|---|---|
| MPPT, Vmax | 10 | 100 | 0.199 | 0.135 | 0.121 | 0.039 | 0 | 61 |
| MPPT, Trickle | 10 | 100 | 0.199 | 0.135 | 0.121 | 0.039 | 0 | 86 |
| Clamp, Vmax | 10 | 104 | 0.181 | 0.136 | 0.123 | 0.014 | 0.08 | 94 |
| Clamp, Trickle | 10 | 103 | 0.182 | 0.136 | 0.123 | 0.015 | 0.08 | 68 |
| Direct Coupled | 10 | 100 | 0.183 | 0.135 | 0.121 | 0.023 | 0 | 52 |
| Minimum SOC | 72 | +/- 15 Ah | | | | | | |

## Table 11 - Undersized Array, Upsized Battery

Module Size = 18 Wp
Battery Capacity (20 hr) = 72 Ah

| | No. Modu | No. Batt | Array (MWh) | Bin (MWh) | Bout (MWh) | Waste (MWh) | Wiring (MWh) | SOCmin (Ah) |
|---|---|---|---|---|---|---|---|---|
| MPPT, Vmax | 9 | 110 | 0.179 | 0.135 | 0.122 | 0.020 | 0 | 362 |
| MPPT, Trickle | 9 | 110 | 0.179 | 0.136 | 0.122 | 0.019 | 0 | 390 |
| Clamp, Vmax | 9 | 114 | 0.162 | 0.130 | 0.124 | 0.002 | 0.08 | 345 |
| Clamp, Trickle | 9 | 114 | 0.162 | 0.131 | 0.124 | 0.002 | 0.08 | 363 |
| Direct Coupled | 9 | 110 | 0.163 | 0.134 | 0.123 | 0.006 | 0 | 345 |
| Minimum SOC | 361 | +/- 16 Ah | | | | | | |

# 5. Development and Implementation of PV-Diesel Model

The design of hybrid PV-diesel generator systems can follow two approaches.

In large autonomous systems for warm climates, the sizing of the array and the battery is done in such a way as to reduce the fuel consumption to a low percentage (≈10%) compared to a pure diesel generator system. [10] The sizing of the system is determined by a minimization technique which balances the fuel savings vs the cost of the array and the cost and lifetime of the batteries.

The second approach, for colder climates (such as northern Canadian sites) is that the diesel generator operates primarily during the winter months when the level of insolation is very low. The generator operates between 12 and 48 hours, recharging the batteries and powering the load. This is followed by a few days during which the batteries supply the load. During the summer months, the array and battery handle most of the energy requirements. The generator is on only a few hours each month, mostly for maintenance procedures.

Figure 8 shows the basic photovoltaic-generator system. In this figure, the energy flows from left to right except for the battery when being recharged. The additional components needed when adding a generator to a photovoltaic system is an AC to DC converter* for charging the battery and a DC to AC inverter for supplying the AC loads when the generator is not on.

The control scheme of this system consists of one ganged set of three switches and two normally closed switches. The switches in Figure 8 are positioned for the photovoltaic array and the battery suppling the DC loads, and the AC loads via the inverter. When the generator is on, the ganged switches will be in their opposite positions and the generator will be supplying the AC loads directly. The switch before the converter is closed when the battery's charge is below the specified fast charging upper threshold (i.e. below the 80% state of charge - SOC) and the switch will be open when the battery's charge is above the upper threshold. The photovoltaic panels trickle charge the battery to its 100% SOC, the battery's switch is then opened to prevent over charging of the battery. When the battery's charge is below the lower threshold, the generator will charge the battery via the converter until the upper threshold is reached. In larger systems, if the AC load exceeds the converter's capacity, the generator will be on. If the battery charge is below the upper SOC threshold, the converter will charge the battery and supply the DC loads.

The three ganged switches ensure that the AC bus is never supplied from the DC bus via the inverter and the generator simultaneously. This eliminates the problem of synchronizing the two AC sources and the unnecessary losses of the inverter. However, this problem also

*A converter simply rectifies AC into DC while an inverter chops up the DC to make AC. The DC regulator is sometimes referred to as a DC to DC converter even though it really is an inverter that chops the DC into a high frequency AC and then converts the AC to DC again.

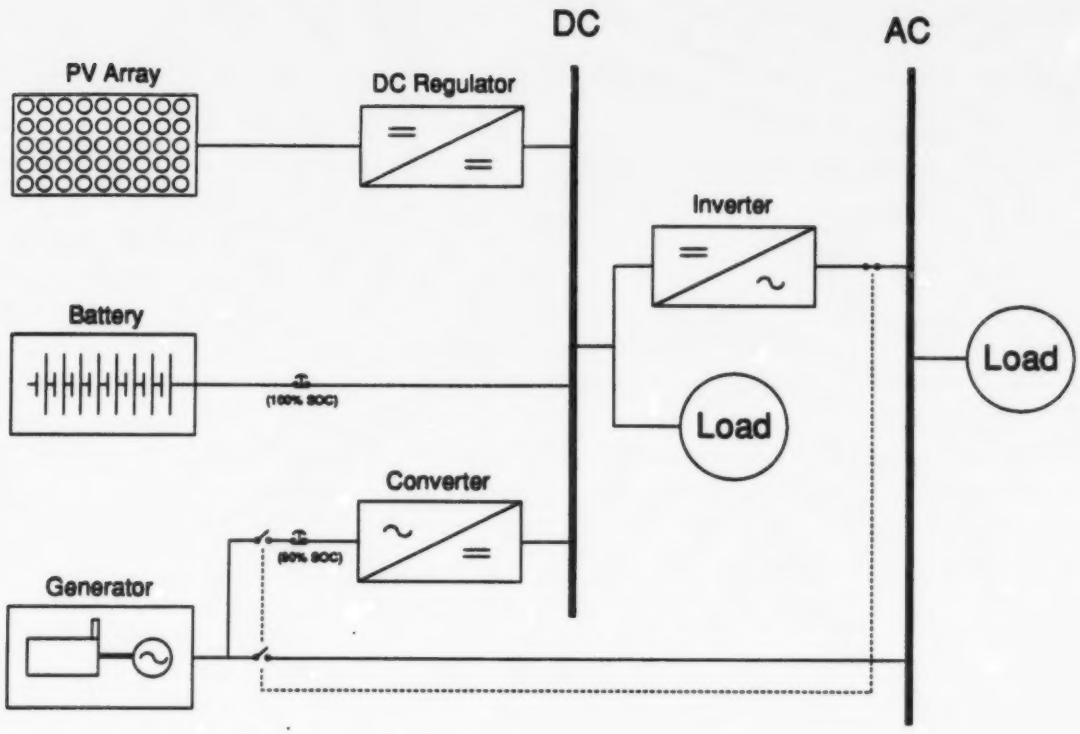


Figure 8 - A Hybrid Photovoltaic-Generator System

exists when switching between the two systems. The simple solution is using fast acting switches (i.e. SCRs or transistors) which operate when the two systems are almost in phase with each other. Serious damage can result and, more likely, a momentary interruption of power will occur if the two systems are out of phase when switched.

In the following sections a more detailed discussion of system components and the requirements for the hybrid model is given.

## 5.1 Diesel Generator Requirements

The two main considerations for the generator are its capacity and the criterion for turning on and off the generator relative to the status of the rest of the system.

### 5.1.1 Generator Capacity

Intuitively, the generator capacity could be less than or greater than the sum of the AC load and the converter. The AC generator is independent of the DC bus since the converter is essentially a fixed load. For a system with loads that are intolerant to power interruptions, the generator's capacity must be greater than the load. To simplify the condition when the

load exceeds the generator's capacity, a portion of the AC load will be shed so that only the maximum power is delivered. The converter load is always met and must be smaller than the generator's capacity for a viable system. The simulation program should report which portion of the AC load is not met. This will be reported also in a more general form to facilitate evaluating the capacity of the generator. The maximum monthly AC power demand on the generator should be expressed in terms of power and as a percentage of the generator's rating. In the unlikely event that the reported maximum AC power is given without the converter load, it should be added to the reported figure or noted. This is needed to avoid presenting results that would significantly change if the weather data for example, is slightly modified.

The fuel consumed by a diesel generator is dependent on the altitude, temperature and fuel type. The fuel efficiency curves will be fitted with the cubic spline routines of the WATSUN-PV program for the profile points (i.e. 5 per profile) and then derated for altitude and temperature. If a different fuel is used, a new profile should be entered by the user or the derating percentage could be combined with the altitude derating factor if necessary.

### 5.1.2 Generator Start/Stop Conditions

Due to the design of the rest of the simulation program, the generator will always start and stop on the hour. When the generator is called for during an hour, the simulation is repeated for that hour with the generator on. This simplification inherently provides a form of hysteresis needed to prevent the generator from cycling on and off frequently.

There are three system states during which the generator would be on.

The first state is when the AC load exceeds the lower of the user specified threshold or the inverter's capacity.* The generator will always turn off when the AC load drops below the threshold. This assumes that the battery's SOC can never drop below the lower SOC threshold when the generator is running since the converter will be on when the battery's SOC is below the upper SOC threshold. This assumption is violated when the DC load, excluding the inverter, is greater than the capacity of the converter. This case is, however, not feasible because the battery will be sooner or later drained by the DC load.

The second state is when the state of charge (SOC) of the battery reaches the lower threshold, ie: battery nearly empty. The generator will supply power to the converter and the AC loads. The converter should be sized to fast charge the battery, and also supply the DC load. This implies that the DC load must be less than the converter's capacity. When the battery reaches the upper threshold the generator will turn off. However if the AC loads exceed its threshold as described in the first state, the converter switch will open and the generator will

*Also the generator will be on when the inverter malfunctions. In the simulation program, this condition is ignored.

continue to operate according to the first state conditions. The array will trickle charge the battery when the battery is not fully charged and when the DC load does not exceed the power from the PV panels.

The third state is after the generator has not been running for a user specified time period (e.g. 2 to 3 weeks) to ensure that the generator will start. During this maintenance run, the generator will supply power for the AC loads and battery charging if necessary.

The major problem in implementing the second state, is to determine the state of charge of the battery. In a simulation, it is easy to calculate the SOC and set the upper and lower threshold for fast charging between for example, the 80% and 20% SOC levels. The SOC is obtained by integrating the current flowing into and out of the battery and compensating for temperature. This calculation can only be implemented with an intelligent controller that also utilizes the battery voltage to verify the battery's temperature adjusted SOC. In practice, the battery voltage corrected for temperature is used to obtain a rough indication of the battery's charge. In the simulation program, the user will have the option to use either the SOC or the temperature adjusted battery voltage. The simulation program will provide both values in the detailed hourly output so the user can get the voltage set points for the controller of the system. In some installations, where reliability is critical, the lower threshold should be raised to provide a safety margin for the inaccuracies resulting from using the temperature corrected battery voltage to indicate its SOC.

The converter may turn off during the simulation hour unlike the DC and AC loads which are constant throughout the hour. The converter is turned off when the battery has reached its upper threshold. The assumption that the converter is on for the full hour probably will result in over estimating the fuel consumption and inefficiencies of the system. One method of handling this condition is to simulate it as being on for half the hour and therefore consuming half its energy. In the unlikely event that the maximum power demand on the generator occurs during the same hour as the converter is turned off, the maximum power must reflect the power level before the converter was turned off.

## 5.2 Converter Requirements

The converter operates at the rated current independent of the loads on the DC bus from its nominal voltage. Its energy demand will fluctuate slightly due to the variation in the DC bus voltage. The converter's current should be sized to meet the DC load and not charge the battery too quickly or too slowly. This implies that the DC load should be small or at most vary over a small range relative to the desired charging rate. The generator only charges the battery through the converter, when the battery's SOC is between the upper and lower thresholds (e.g. 80% and 20%). The array can charge the battery between the fully charged and lower thresholds (e.g. 100% and 20%) if all its energy is not used by the DC loads or inverter.

## 5.3 AC Load Requirements

Typically, the AC load will be the major load on the system. Besides the daily and hourly fluctuations in the AC and DC loads, the AC load can be adjusted each month to reflect seasonal load demands.

When the AC load exceeds the user specified level, the generator is started. It will stop when the AC load drops below the threshold. This threshold must be less than or equal to the inverter's capacity otherwise the inverter's capacity becomes the threshold.

When the AC load, which can include the converter, exceeds the generator's capacity, the simulation program will first supply the converter and than part of the AC load up to the generator's rating. In practice, if load shedding is feasible, multistage load shedding is done based on a hierarchy. The remaining loads that can not be shed must be less than the generator's capacity. The approximation of delivering 100% of the generator capacity is accurate enough for the simulation. The important issue is the monthly maximum demand on the generator. This demand includes the loads which were shed and the converter even if it was not on at the time. This demand is needed to determine the sizing of the generator for the given battery and photovoltaic system sizes.

## 5.4 Input Specifications

In order to integrate the PV-diesel model into the existing photovoltaic simulation program input specifications are required. The input specifications that the user must supply or modify from the default design and the fundamental equations relating the parameters are given below.

**G - Generator**

| | |
|---|---|
| AC Line Voltage | V |
| Continuous Power Rating | kW |
| Fuel Consumption vs Load (Profile) | L/Hr/% load |
| Altitude | m |
| Altitude Derating (Profile) | %/Altitude |
| Temperature Derating Gradient | %/°C |
| Derating Reference Temperature | °C |
| Maximum Interval for Maintenance Run [0 = no runs] | Hrs |

Calculation Steps:

1) % AC Load: $\frac{Power}{Continuous\ Power\ Rating} = \%Load$

2) Fuel Efficiency: calculate the kWh/L from the fuel curves

3) Overall Efficiency $FuelEff \times (100 - (Altitude\ Derating \times Altitude)) \times$

$(100 - (Temp\ Derating \times (Ref.Temp - Temp)))$ [%]

4) AC Energy: $Power \times Time = Energy$ [kWh]

5) Fuel Consumption: $Energy \times Overall\ Efficiency$ [L]

**A - AC Load**

| | |
|---|---|
| AC Voltage | V |
| AC Load Threshold to Start Generator | W |
| Number of days in "weekdays" | # |
| Number of days in "weekends" | # |
| Max AC Load for "weekdays" | W |
| Max AC Load for "weekends" | W |
| Profile - Fraction for "weekdays" | %,%,%,%,%,%,% |
| Profile - Fraction for "weekends" | %,%,%,%,%,%,% |
| Seasonal Profile Adjustments (monthly) | %,%,%,%,%,%,%,%,%,%,%,% |

Calculation Steps:

Required Load:

Max $Weekday\ Load \times Weekday\% \times Month\% = AC\ Load$ [kW]

or

Max $Weekend\ Load \times Weekend\% \times Month\% = AC\ Load$ [kW]

**C - Converter (AC to DC)**

| | |
|---|---|
| AC Voltage | V |
| Nominal DC Voltage | V |
| Current Rating | A |
| Efficiency | % |
| Generator Start Method (SOC or V) | 0/1 |
| Temperature Compensation of V | V/°C |
| Generator Start (SOC or V) | % or V |
| Generator Stop (SOC or V) | % or V |

Calculation Steps:

AC Bus Converter Load (assuming fixed current output):

$$\frac{DC\ Current \times DC\ Bus\ Voltage}{Efficiency} = AC\ Inverter\ Load\ [W]$$

**I - Inverter (DC to AC)**

| | |
|---|---|
| Nominal DC Voltage | V |
| AC Voltage | V |
| Inverter Power Rating | W |
| Inverter Efficiency (Profile) | %/% load |

Calculation Steps:

1) Percent Inverter Load: $\frac{AC\ Load}{Inverter\ Power\ Rating}$ [%]

2) Inverter Efficiency: calculated efficiency from load curves

3) DC Bus Inverter Load:

$AC\ Load \times Efficiency = DC\ Inverter\ Load\ [W]$

## 5.5 Printout Additions

Table 12 lists definitions for ten possible monthly output columns that could be included in the output printout.

Table 12 - Output Printout

1) Generator Output [MWh]
2) Fuel Consumption [L]
3) Peak Generator Power Demand [W]
4) % Peak of Generator Capacity [%]
5) Average Load When Running [% of generator capacity]
6) Average On Time per Start [hrs]
7) Monthly Running Time [hrs]
8) System Losses [MWh]
9) % of DC Load from PV [%]
10) % of AC Load from PV [%]

In a photovoltaic system, energy losses are important. In generator only systems, however, losses are often ignored. The system energy losses occur in the battery, wiring, DC regulator, AC to DC converter, inverter and generator. These losses are lumped together as system losses, as they are not quite as important as in the basic photovoltaic system.

Applications of the PV-diesel model will be introduced in chapter 7. together with the battery aging model described in chapter 6..

# 6. Development and Implementation of Lead-Acid Aging Model

The consideration of battery aging in a PV system is important from a number of points of view. Accurate knowledge of the expected life of a battery under a set of operating conditions allows batteries to be replaced before operational failures occur. Such failures may be a result of the sharp drop in capacity towards the end of battery life, or due to catastrophic cell failure.

Incorporation of a battery aging model into a PV system simulation provides the designer with the ability to determine the effect of component sizing upon the battery discharge regime, and consequently the effect upon battery life. The expected battery life is a major component in any economic model of a PV system. Furthermore, the requirement for preventive maintenance may be estimated. For remote systems, this information is invaluable.

Battery service life has two components, cycle life dependent upon the charge-discharge regime, and a calendar life independent of cycling. Generally, service life is limited by cycle life.

## 6.1 The Process of Aging

There are a number of design and operating parameters that have a strong influence on battery life. From the point of view of cell design, cell life ranks as a significant consideration along with cell efficiency, and energy to weight ratio. The design of a battery is beyond the scope of this work, consequently only consideration of operating parameters will be made.

The reader should note that the electrochemistry discussed in this section is extremely simplified for the purposes of clarity and brevity. For a good overview of battery chemistry the reader should consult references [11-13].

Operating parameters that are considered significant are depth of discharge, relative rate of cycling, operating temperature, storage temperature, and effectiveness of charge control.

Depth of discharge affects battery life in two ways. First, each discharge-charge cycle is not completely reversible. Every cycle and its relative depth reduces the life of the battery by a small but finite amount. Figure 9 depicts the relation between depth of discharge and cycle life. The amount of time a battery remains at a low state of charge affects its useful life also. Second, the depleted electrolyte in a battery at a low state of charge is extremely corrosive, promoting the formation of lead sulphate; its effect will be discussed in detail below.

Increasing the rate of cycling that a battery experiences contributes to a reduction in battery life. The rate of cycling is dependent upon charge and discharge rates. Rapid cycling requires high currents, which may damage the cells of a battery through heating, promotion of incomplete reactions, and a number of other minor effects.

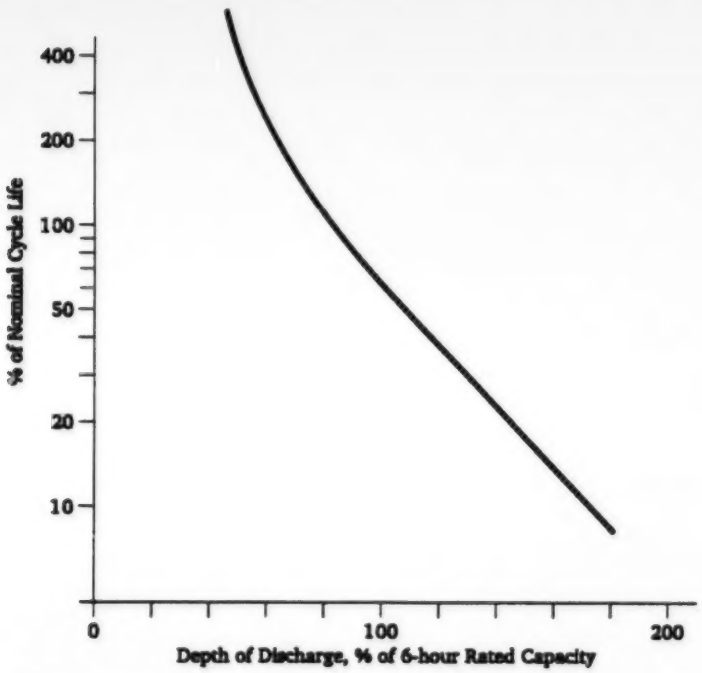


Figure 9 - Battery Cycle Life vs Depth of Discharge
Adapted from Handbook of Batteries and Fuel Cells [14], Figure 14-34

The operating temperature of a battery can be in certain cases the most significant factor leading to the accelerated reduction of the operating life. Figure 10 shows a typical dependency of life on temperature.

As temperature increases, so does the rate of corrosion, the rate of self discharge and the solubility of metallic components. An increase in self discharge necessitates an increase in charge input to restore charge capacity. The increased charge input is also heavily consumed by electrolysis reactions, producing hydrogen and oxygen gas. Incomplete charging is common, leading to a severely reduced capacity. Increased gas liberation results in an increased requirement for electrolyte level maintenance.

At low temperatures the battery is in danger of freezing, particularly at low states of charge. At 100% SOC, the electrolyte freezing point is approximately 70°C, while at 0% SOC, the electrolyte will freeze at approximately 10°C.

Storage of a battery at elevated temperatures leads to rapid self discharge to a low SOC, subsequently corrosion and irreversible sulphation render the battery dead.

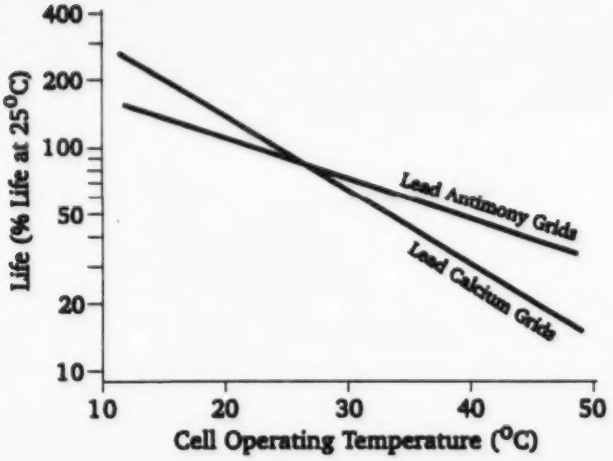


Figure 10 - Effect of Temperature on Battery Life
Adapted from the Photovoltaic System Design Handbook [15], p.7-35

The charging of a battery must be closely controlled to ensure complete recharge with a limited and tolerable level of electrolysis (gassing). Excessive gassing will necessitate increased maintenance. Incomplete charging directly reduces the available capacity, and may on a short term basis lead to memory effects in a lead acid cell. Stationary batteries, as used in a PV system, require a controlled amount of overcharge and gassing to overcome electrolyte stratification - a process whereby more concentrated electrolyte accumulates at the bottom of the cell.

## 6.2 The Aging Model

Consider the conditions experienced by batteries in PV systems in a typical Canadian site.

The average operating temperature of a battery exposed to outdoor conditions is generally below 20°C, consequently high temperature aging effects are less significant. Batteries may experience extended periods below 0°C, a region in which freezing may take place. The relatively extreme range of temperatures possible (-40°C to 30°C) present difficulties for precise charge control since charging requirements change with changing temperature.

Batteries in remote locations may be required to operate for extended periods without maintenance. The sunshine regime of most Canadian sites and the specifics of each system could potentially result in a significant amount of charge-discharge cycling.

The aging model formulated for WATSUN-PV, is a passive one; it tracks the aging of a battery but does not modify the characteristics of the battery with age. At the end of an annual simulation the reduction in life and other useful parameters are reported to the user. The passive approach is justified in that the greatest effect of age is upon capacity. Capacity

does not drop significantly until 80% of life, as illustrated in Figure 11. Most batteries, in service in PV systems would have an actual cycle life well in excess of 1 year which is the length of most simulations.

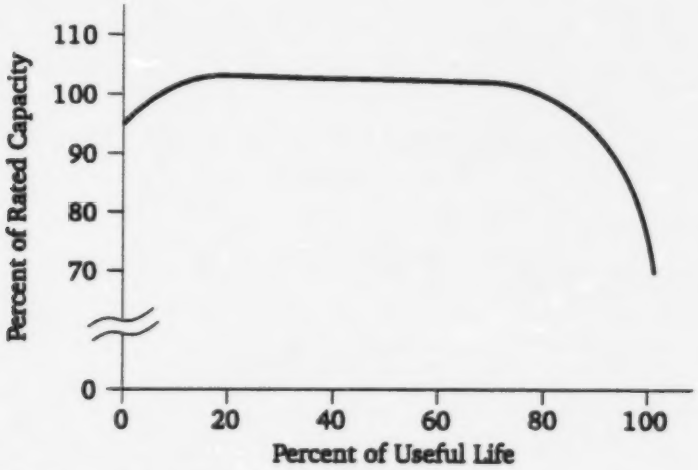


Figure 11 - Typical Battery Capacity Curve
Adapted from the Photovoltaic System Design Handbook [15], p.7-21

Due to typical Canadian site conditions, the influence of high temperatures on aging is not modeled. This and other effects could be eventually incorporated into a high temperature model of batteries to make WATSUN-PV internationally acceptable.

As shown in Figure 10, the life of a battery is increased over the nominal life as the temperature decreases below 20°C. Consequently, neglecting this effect in the model will yield conservative results. A possible life-temperature model is proposed later. Low temperature effects (ie freezing) are dealt with in the battery model itself.

The effect of cycle aging is modeled by tracking charge and discharge cycles; decrementing life accordingly. The effect of overcharging is modeled by tracking the amount of gas evolution in the battery model. Any known limit in the calendar life of a battery is used as a limiting mechanism during hours of low cyclic activity.

Each component of the model is discussed in detail in the next section.

### 6.2.1 Cycle Life Component of Aging Model

The cycle life component is built around the cumulative wear or deterioration process that charge-discharge cycles cause. This action may be understood by consideration of the electrochemical process involved.

Upon discharge, the lead (Pb) of the negative electrode, and lead dioxide ($PbO_2$) at the positive electrode are converted to lead sulphate ($PbSO_4$). The charging process does not re-convert all of the $PbSO_4$ to $PbO_2$ and Pb. With each cycle, small but finite amounts of $PbSO_4$ and $PbO_2$ become detached from the electrodes. This process occurs predominantly at the end of charge and beginning of discharge, and is affected by rate of charge, discharge and gassing.

The initial effect of this action is to reduce the availability of active Pb and $PbO_2$. Cells are designed with a surplus of active material, and as long as these reactants are in abundance, the process does not have a significant effect upon battery performance. The battery capacity will drop marginally over the bulk of its life as a sulphate and dioxide "sludge" accumulates in the cell.

Eventually, the surplus of Pb and $PbO_2$ becomes exhausted; the cells capacity begins to drop faster with each cycle. This is the normal end of life point for a battery. Chemically the battery is exhausted.

Figure 9 depicts the typical effect of cycle depth upon cycle life. For a given cycle depth, say 100% of the 6 hour rated capacity, the cycle life would be 55% of nominal rated life. The nominal life in this case is at a depth of discharge 80% of the 6 hour capacity. 80% of the 6 hour capacity would be close to the 10-20 hour capacity.

Given a number of cycles at a certain depth of discharge, and the actual cycle life from Figure 9, the percent of life the battery is at may be determined. Using Figure 11 the rated capacity may be derated with age.

The increase in capacity of the battery over the first 10% or so of its lifetime, is a result of the "formation" of reactants. Initially, although there is an abundance of reactants (Pb, $PbO_2$), they must be activated, or "formed" by charge and discharge cycling. This is commonly thought of as battery break-in.

In most photovoltaic systems, a battery does not experience multiple cycles at a fixed depth of discharge. Generally the battery is required to cycle irregularly daily, monthly, and in some cases annually, with smaller sub-cycling induced by load demand and solar resource availability.

In the case of a photovoltaic-diesel hybrid system, the battery will experience very rapid charge from generator output, with gradual charge and discharge from the array and load current. Typical charge-discharge regimes are portrayed in Figure 12.

In order to accommodate patterns of irregular cycling, it is necessary to consider the actual cycle pattern as composed of small but finite regular cycles. In isolation, each of these cycles is regular and characterized by a change in SOC usually less than 100%.

The relationship represented by Figure 9 may be restated in terms of the reciprocal of nominal cycle life, or the amount of life used per cycle, given in Figure 13

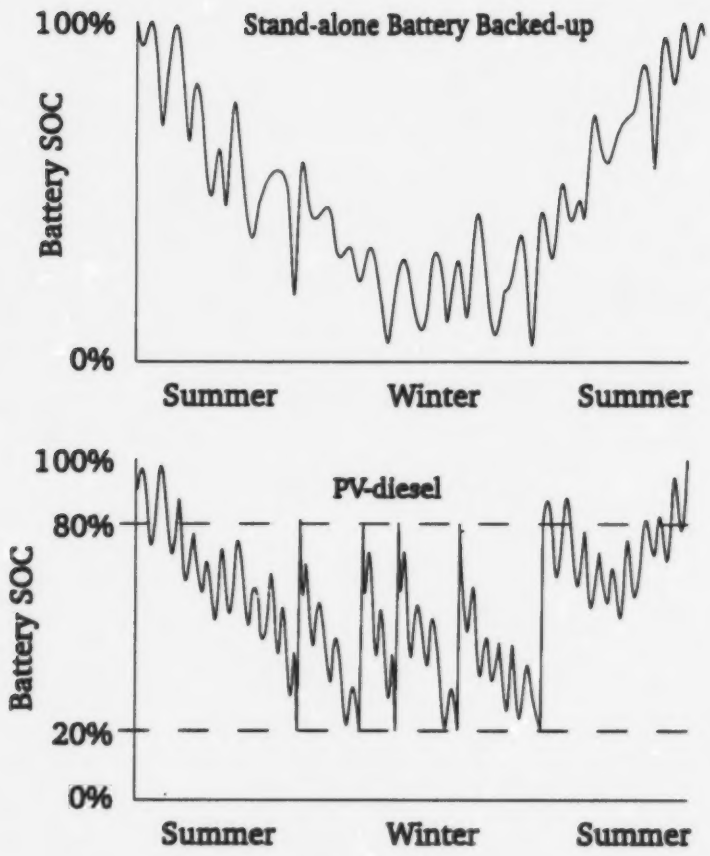


Figure 12 - Typical Charge-Discharge Regimes

Subsequently, by differentiation of this function, another function relating the change in life for an incremental change in state of charge (dL/dSOC) as a function of state of charge (SOC) is derived as illustrated in Figure 14. Given a state of charge, SOC, and a small cycle depth dSOC, the change in life dL may be computed. The quantity dL is dimensionless. If in one hour the term dL is 0.0000228, the life of the battery under the same conditions would be the reciprocal or 43,800 periods. For the hourly period, this means the cycle life would be 43,800 hours, or 5 years.

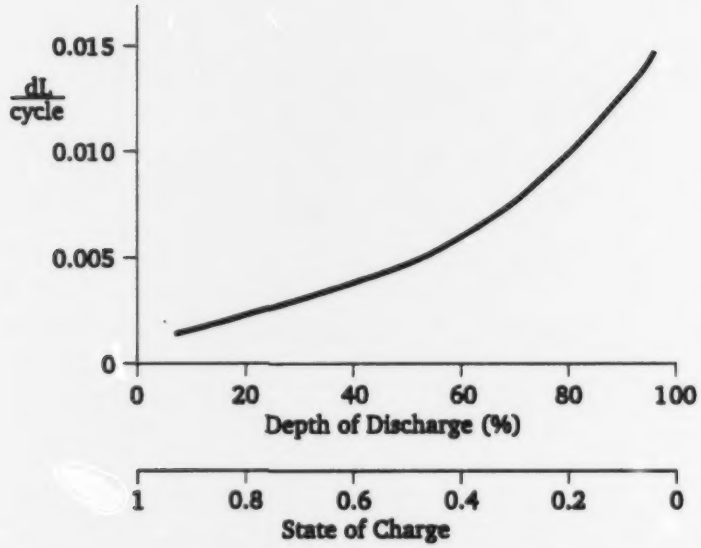


Figure 13 - Change in Battery Life per Cycle

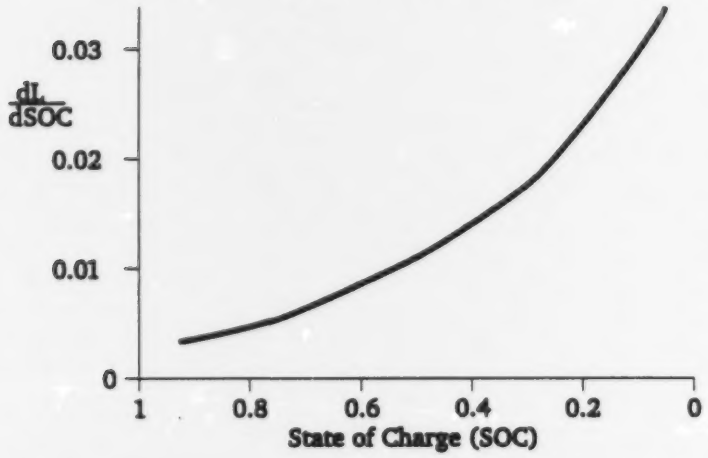


Figure 14 - Cycle Life Reduction Function

Since the battery wear is related directly to the ionic exchange that takes place, the aging model is based upon the absolute state of charge in coulombs. This is in contrast to most other components of the battery model which use the relative (temperature adjusted) state of charge. A consequence of this assumption is that it may be more difficult to wear out a cold battery because the more taxing ranges of absolute state of charge cannot be reached.

Regardless of how little cycling occurs, there is an upper limit on the calendar life of the battery. This corresponds to the case where a steady low level charging current, just sufficient to overcome self-discharge, is applied. At this point in the simulation we can determine whether this mechanism will play a dominant role for the hour. If a battery has a calendar life of $N_C$ hours, then as each hour passes it looses $1/N_C$ of its life. If $1/N_C$ is greater than the dL due to cycling then the battery will age more due to time. On the other hand if dL is greater than $1/N_C$, then the cycling regime of the battery will dominate the aging process.

As illustrated in Figure 14 the function dL/dSOC(SOC) herein referred to as "cycle life reduction function" is non-linear in state of charge. Aside from the effect of absolute magnitude of the discharge cycle, this function takes account of the absolute state of charge at which the cycle takes place. In short, the function predicts that a cycle between 100% and 80% SOC does not reduce the battery life to the extent that one between 60% and 40% SOC would.

#### 6.2.1.1 Implementation of the Cycle Life Component

Given the cycle life reduction function, implementation within an hour-by-hour simulation model is straight forward. For each hour the effective charge-discharge cycle that the battery experiences is used to determine the net reduction in cycle life (the quantity dL). This value is then compared to the aging as a result of time (the quantity 1/N). The greater of these two values is taken as the reduction in battery life for that hour. Over the course of the simulation this value is accumulated.

Consider the simple, but irregular cycles illustrated in Figure 15. Four hours in the life of a battery are represented. At the beginning of the 1st hour and end of the 4th hour, the battery is at 100% SOC. At the end of hours 1, 2, and 3, the battery is at 60%, 80% and 30% SOC respectively. Three complete discharge-charge cycles can be identified in this pattern, although the two halves of each cycle are not necessarily contiguous. Each cycle is labelled on the figure with a two letter code, the first letter in lower case being a d or c for discharge or charge and the second letter in upper case identifying which of the three cycles. The three complete cycles are: dA-cA, dB-cB and dC-cC.

The change in state of charge, up or down, in each hour represents 1/2 of each of the 3 cycles. Each complete cycle may be characterized by an average state of charge for the hour. For each cycle the reduction in life may be predicted by the cycle life reduction function, given the average state of charge, and the depth of the cycle.

Practically, within the simulation, only one half of each cycle is encountered during each hour, therefore, the cycle depth used in the evaluation of the cycle life reduction function is 1/2 of the actual change in state of charge for the hour. Table 13 illustrates the progression of the simulation.

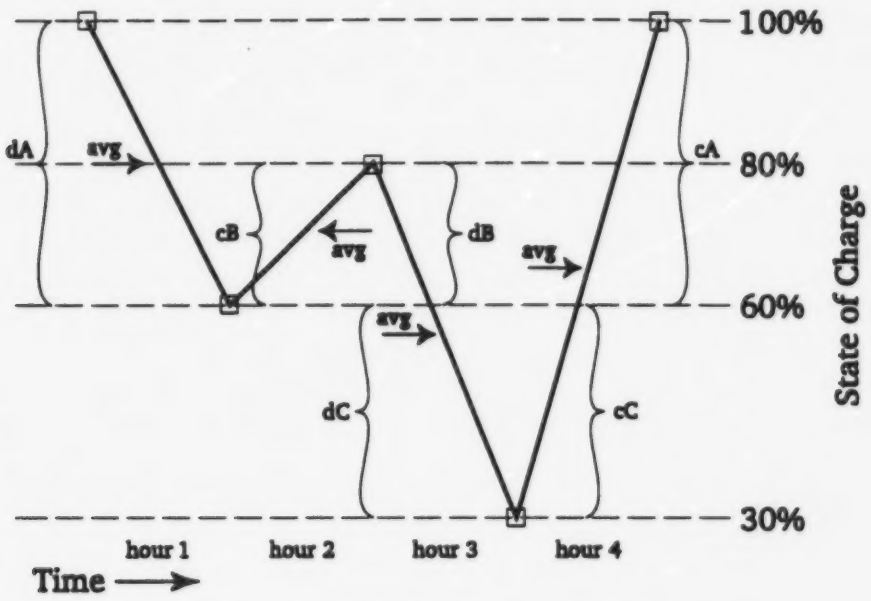


Figure 15 - Sample Hourly Battery Cycles

Table 13 - Simulation Tabulation

| | | ---- Depth ----- | | |
|---|---|---|---|---|
| Hour | Cycle | Actual | Effective | @SOC |
| 1 | d-A | 40% | 20% | 80% |
| 2 | c-B | 20% | 10% | 70% |
| 3 | d-B + d-C | 50% | 25% | 55% |
| 4 | c-C + c-A | 70% | 35% | 65% |

### 6.2.2 Gassing (Electrolysis) Component of Aging Model

Gassing is the other component of the aging model which strictly speaking is not actually an aging function. This is the process whereby hydrogen and oxygen gas is evolved from water in the electrolyte at the end of the charge cycle.

This effect is dealt with in detail in the battery model presented in section 3.2. Consequently, we will limit our discussion to the reporting function implemented.

Within the battery model, the amount of current resulting in gas production is determined as a consequence of predicting the amount of current contributing to useful charge. For each hour it is possible to derive the number of amp-hours lost to gassing; this is converted to a volume of gas produced, and consequently the amount of water lost.

The model simply reports the accumulated amount of water lost from the battery over the course of the simulation. This is useful for both the modeling of maintenance free and vented batteries with or without gas recombination systems. In the case where recombination is available the model provides for a tolerable level of gassing not resulting in water loss.

Prediction of the amount of water consumed will allow a designer to predict the need for maintenance in the case of a vented battery, and predict, in the case of a maintenance free battery that the charge regime the battery will be subjected to, will likely lead to its demise.

## 6.3 WATSUN-PV Aging Model Input

The following information is required to use the battery aging model in WATSUN-PV:

Cycle Life Model

Nominal Cycle Life measured in number of cycles - a single valued parameter.

Nominal Cycle Depth in (%) of nominal battery capacity - a single valued parameter.

Calendar Life in years - a single valued parameter, representing the maximum calendar life regardless of charge discharge cycle regime.

Aging Calculation On/Off Switch - a single valued parameter. Allows the user to disable the aging model.

A function relating Cycle Life (# of cycles) to the Depth of Discharge (%) - a five valued profile, that the model uses to derive the cycle life reduction function. The depth of discharge is in terms of the nominal cycle depth, while the cycle life is in terms of the nominal cycle life. A default function is provided that is typical of lead-acid batteries. It should be noted that this function is not necessarily coupled to the nominal values given above. The simulation will scale this function to ensure the nominal values lie on the curve.

Gassing Model

Electrolyte Volume measured in litres. A single valued parameter allowing the model to report, percent of electrolyte lost, or if zero, to report amount of electrolyte lost.

Recombination Rate measured in $cm^3$/hour - single valued parameter.

A gassing function (current vs. voltage) is provided as part of the battery model, and is utilized by the gassing model.

All of the above information should be readily available from a battery specification sheet, or directly from the battery manufacturer. Since the model is passive in nature, any inaccuracies inherent will not affect the accuracy of the other parts of the simulation model. This feature is intentional, as data on battery life is generally statistical in nature. Any given battery may perform significantly different in terms of service life.

## 6.4 WATSUN-PV Aging Model Output

For each month, and on an annual basis the cycle life model reports the predicted life used on the basis of the cycle regime for the time period, and the amount of life remaining after the period (month or year).

A typical output is given in Table 14.

Table 14 - Aging Model Output

| Month | Life Used |
|---|---|
| Jan | 1.57% |
| Feb | 1.81% |
| Mar | 1.24% |
| Apr | 0.94% |
| May | 1.10% |
| Jun | 1.07% |
| Jul | 1.44% |
| Aug | 1.23% |
| Sep | 1.28% |
| Oct | 1.16% |
| Nov | 1.41% |
| Dec | 1.32% |
| Year | 15.57% |

Life expectancy under present conditions is 6.4 yrs.
80% of battery life will be reached in 5.1 yrs.

This should be interpreted as follows: the battery would reach 100% of its expected life in 6.4 years from commissioning if the present cycling regime prevailed. Since the battery capacity drops significantly after about 80% of service life, the battery should be replaced after about 5.1 years has elapsed.

The gassing component of the model reports:

Total volume of water lost to gassing is 10 litres.
OR
12% of electrolyte volume lost to gassing.

If the input specifies electrolyte volume, a percentage is reported, otherwise, a volume is reported.

## 6.5 Proposed Incorporation of Temperature Effects

Should further research and battery testing suggest that it is not prudent to neglect the effects of temperature upon battery aging, the following method could be used to incorporate these effects into the model:

1) Document the effect of temperature (low and high) upon total battery life (similar to Figure 10)

2) During each hour proceed with the determination of the reduction in life (dL) for that hour as described above.

3) Apply a factor based on the data assembled in 1) to the quantity dL, to account for the incremental affect of the temperature for that hour on the batteries life.

4) Accumulate the dL value as presently done.

This approach should allow the user to account for different sensitivities to temperature demonstrated by various types of batteries.

# 7. Application of New PV-Diesel and Aging Models Using WATSUN-PV

The PV-diesel and aging models have been implemented in WATSUN-PV 3.0. Watsun will run simulations after the program has been fully debugged. Here we present the procedures for the possible simulations along with their motivation and anticipated results. The actual performance of these procedures can be used by Watsun in the verification of the new models.

In these simulations, usually one or more particular sites are chosen with specific meteorological conditions, load requirements and sizing of the diesel generator if present. Then the key input variables to each simulation run are the array and battery sizes. The key output variables are the minimum temperature adjusted battery state of charge for the year, the frequency and duration of generator usage and the degree of battery aging and maintenance required. The majority of these investigations at some point involve an iterative sequence of simulations seeking a battery and array sizing that achieves a particular minimum state of charge without any load shedding and therefore a corresponding "margin of reliability". The simulation variables are illustrated in Figure 16.

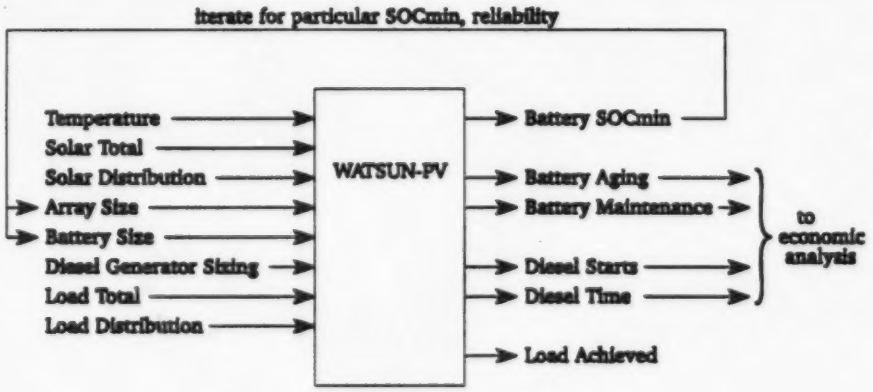


Figure 16 - Key Simulation Variables

## 7.1 Application of Aging Model

Simulations will be performed on two remote stand-alone systems exposed to the same total available array energy, but very differing annual energy distributions. One will be at a southern Canadian site with a battery charge/discharge cycle of the order of days while the other will be at a far northern site with an annual charge/discharge cycle. The system load requirements will be identical.

Using iterative simulations, the two systems will be sized to achieve the same minimum temperature adjusted battery state of charge and thus margin of reliability. See Figure 17. The northern site will require a much larger battery both because of the much longer discharge period and because of the low operating temperature. However, it can be anticipated that the battery at the northern site will last much longer because both the frequency of discharge and absolute depth of discharge will be less. (At colder temperatures, a given temperature adjusted state of charge corresponds to a much higher absolute state of charge.) This simulation will determine the degree to which this is true and also give an indication as to the required frequency of battery maintenance (topping up the electrolyte) for non-maintenance-free batteries. For maintenance-free batteries, loss of electrolyte may under some conditions be the limiting factor in battery life.

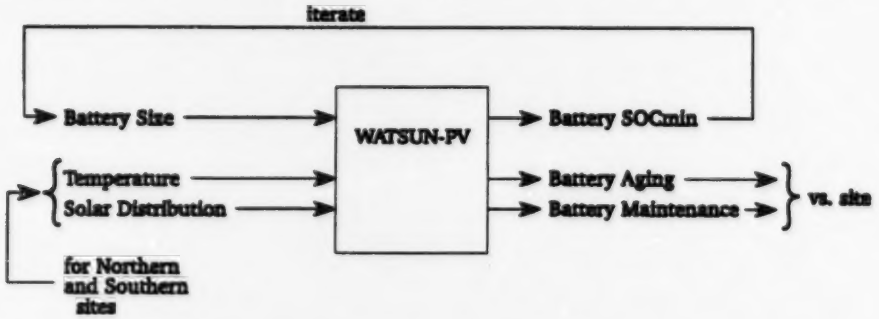


Figure 17 - Aging vs Site

In a series of additional simulations, the battery size in both the northern and southern systems will then be varied to determine the effect on battery life. See Figure 18. The results of these simulations can then be used to perform a long-term economic analysis of the worth of oversizing the battery.

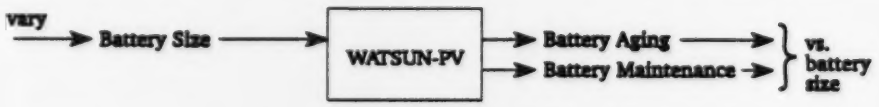


Figure 18 - Aging vs Battery Size

Finally, to examine how errors in the estimation of load or available radiation may contribute to premature battery failure, two series of simulations will be performed on both of the original sites, rescaling the load or array over a range of values. See Figure 19.

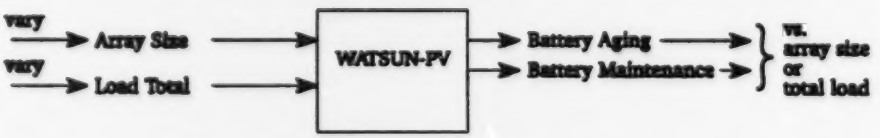


Figure 19 - Aging vs Array and Load Sizing

## 7.2 Application of PV-Diesel Model

Inclusion of a diesel generator in a PV-battery system is particularly cost effective when there may be occasional significant periods of particularly low array energy or occasional peak loads well in excess of the nominal level. In either of these situations, a PV-battery system operating stand-alone would require a considerably greater sizing of the array and battery in order to assure reliable operation. Comparative simulations will be defined for both of these cases.

These simulations will also make use of the battery aging model.

### 7.2.1 Flat Load Profile

A series of simulations will be performed focusing on systems where the primary motivation for use of a diesel generator is to compensate for occasional excessively low available array energy. The aim is to investigate how the overall capital and operating costs relate to appropriate battery and array sizing in a PV-diesel system.

The simulations begin with a reference case. The reference simulation is of a system at a southern Canadian site exposed to a moderately variable radiation pattern. The system is sized so that the diesel generator is not required to run at any point through the year, but is otherwise fairly critically sized. See Figure 20. A series of additional simulations are then performed with a range of battery sizes, all of them smaller than that of the reference. See Figure 21. The simulation results of interest are the number of diesel start-ups, the total hours of operation of the diesel and the percentage of battery life consumed, all expressed as a function of battery size.

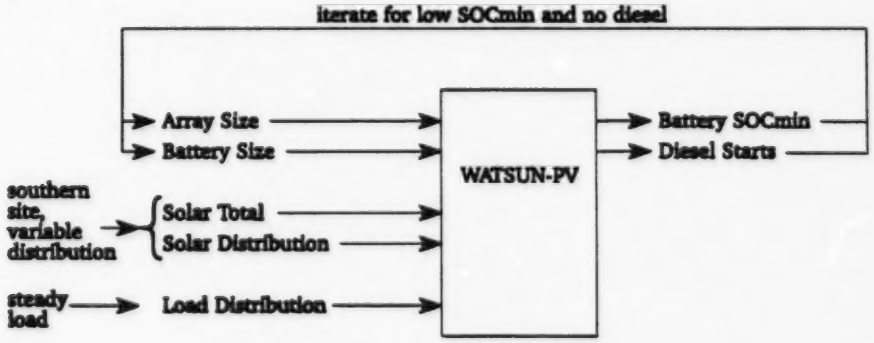


Figure 20 - PV-Diesel Reference Case

The results acquired can be used in an economic analysis to examine the sensitivity of the overall system costs to correct battery and array sizing in a PV-diesel system. The cost of the diesel operation can be determined from the number of start-ups (since each has a cost

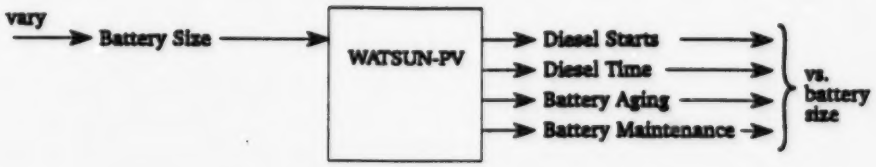


Figure 21 - Diesel Usage and Battery Aging vs Battery Size

penalty) and total run time. The capital and operating cost of the battery can be determined from its size and the aging characteristics. The amortized annual costs of the battery and the diesel operation would then each be plotted as a function of selected battery size.

The sizing of the original reference system is such that the generator is never required to run, but is otherwise fairly critically sized. Any of three conditions can cause the generator to run. One is the AC portion of the load exceeding a setpoint (beyond which the inverter would have been incapable of supplying power). A second condition is the temperature adjusted battery state of charge dropping below a set point; at that time the diesel is run until the battery is 80% recharged. The third condition involves the battery equalization schedule. In the reference system, the diesel is prevented from running by: a) having no AC load component and a relatively constant DC component; b) sizing the array and battery such that the minimum temperature adjusted state of charge is above that which triggers diesel start up; c) disabling the battery equalization schedule.

### 7.2.2 Irregular Load Profile

Another series of simulations similar to the above will be performed, this time with a system where the primary motivation for the diesel generator is to deal with an occasionally large load. Again the aim is to investigate how the overall capital and operating costs are affected by appropriate battery and array sizing in a PV-diesel system.

The reference case will be similar to that of the previous series of simulations in that the system will be sized so that the generator never runs. It will differ from the previous reference case in that the DC load profile will have occasional large peaks which although contributing little to the total yearly load requirements will necessitate a very large battery to assure reliable operation without operation of the generator. See Figure 22. The battery charger will also be radically upsized to enable the peaks to be supplied by the generator in subsequent simulations.

As before, a series of additional simulations are then performed with a range of reduced battery sizes. See Figure 23. The simulation results of interest are the number of diesel start-ups, the total hours of operation of the diesel and the percentage of battery life consumed, all expressed as a function of battery size. The economic analysis is the same as before but this time providing information on the advantages of the use of the diesel generator in dealing with systems with large load spikes.

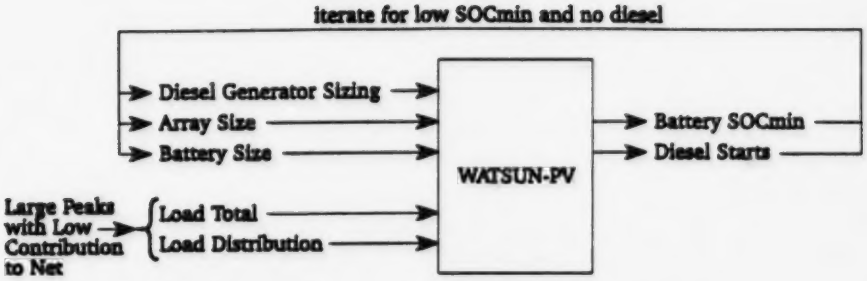


Figure 22 - PV-Diesel Variable Load Reference Case

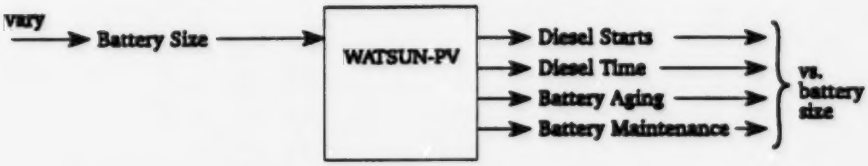


Figure 23 - Diesel and Battery vs Battery Size, Variable Load

# 8. Conclusions

The work described in this report is a significant contribution to the understanding of the interaction among the different components of PV-hybrid systems and the overall system performance.

The basic PV system with battery back-up described in WATSUN-PV was expanded by the development of better models describing the PV array and the battery. Temperature and aging effects on batteries and the inclusion of a diesel generator were also modeled. These enhancements resulted eventually in a new version of WATSUN-PV, i.e. WATSUN-PV 3.0.

Comparison of five different system control strategies was done for a specific site in northern Canada. The margin of reliability of the system, defined as the minimum remaining obtainable charge in the battery was surprisingly strongly dependent on array size. No major differences in system performance were observed due to the control strategy adopted. The maximum power point tracked system required less storage while the trickle charger did not make an efficient use of the energy provided by the array. Both the clamped and direct coupled systems performed approximately the same. The lack of charge regulation did not appear to affect the system ability to satisfy the load requirements. Similar results were obtained by reducing the array size and increasing the number of batteries. The choice of a particular strategy is therefore economic in nature, once a decision is made on the types of array and batteries to be employed.

The simplest way of comparing the various control strategies would have been to simulate them on five identical systems. In practice however, several factors are important when selecting how the system will operate. Cost of implementing a particular strategy is critical. Therefore, the comparison was done by resizing each system to yield the same performance in terms of reliability and load met. Any comparison is then based on component sizing and the corresponding costs. This iterative process was more time consuming but offered results that can be used directly in an economic analysis of the system.

The battery continued to be the most complicated component of the system because of its functional dependence on previous history. In the new model the only characteristics not included were those of short term duration or whose magnitudes were very small. Battery self-discharge and self-heating were thus not included. Stratification and unequal cell performance were not considered either. The life of the battery or aging effects were treated separately in a model. This provides the designer with the tools to determine the effect of component sizing on battery discharge and life.

The acceptance of WATSUN-PV 3.0 by the industry will be dependent on a wide distribution of the software to users and designers of systems. Further improvements should be realized by a combination of the work that remains to be done and the experience gathered by third parties in applications to real systems.

# 9. Recommended future work

The issues raised in this report and discussions held with members of the industry suggest several areas where further work may be appropriate.

## 9.1 Recoding in Pascal

Several interested parties have emphasized the importance of WATSUN-PV being as user friendly as possible. Implementation of user interfaces is generally more easily done in Pascal or C than in Fortran. In addition, a programming environment such as Borland's Turbo Pascal provides a more powerful programming and debugging environment and this would assist both Watsun and other users who choose to work with and customize the source code of Watsun-PV. The more modular nature of Pascal will facilitate a well behaved integration of code from multiple contributors and the use of Watsun-PV code in other applications. The utility of the battery model for example may extend well beyond photovoltaic applications.

Despite an ongoing interest by all parties to recode the software in Pascal, there has not yet been sufficient opportunity to pursue this goal.

If the decision is made to recode portions of Watsun-PV into Pascal, all of the meteorological code would be left as a unit written in Fortran. The code most directly related to the physical model of the PV system (PV array, battery, load, generator, etc.) would be recoded in Pascal, each as distinct, well defined modules. This would be a relatively straightforward task. The user interface, including system parameter editing, would be redesigned extensively. This would be a moderately large task, but would yield a program that far more people would use to a significant degree.

## 9.2 High Accuracy Battery Characterization

The battery continues to be the single most difficult component to model accurately. Unlike other components with a more or less instantaneous response or at least a very predictable time dependence, the battery has a multifaceted time-dependence and is consequently very difficult to characterize accurately over a broad range of conditions.

The battery model of Watsun-PV will continue to be an important focus for further significant model enhancement.

It may also be advantageous for future program development to set up a semi-automated, high accuracy battery test rig. It is clear from the battery testing to date that repeatability is the crucial factor needed for distinguishing the fundamental battery characteristics from the large sample and run specific variations. Once set up, highly repetitive battery cycling could be carried out with a minimal long term expense.

The tests themselves are relatively simple. Individual cells will be used to eliminate the masking of information by unsynchronized cell activity. Temperature will be tightly controlled at several different values. At any given instant, either current or voltage will be strictly controlled while the other is carefully monitored. The flowrate of cell gassing during the latter stages of charging will be measured. The cell will be taken through many charge-discharge cycles until repeatability throughout the cycles is achieved.

The results of the tests will be used both to refine the fundamental mathematical model structure for the battery and secondly to improve the default battery parameters. In practice, the majority of users will probably use the default battery parameters at least as a starting point and subsequently with minimal modification.

## 9.3 Battery Testing for Aging Models

Any additional battery testing should be extended to include aging effects as well.

As part of this contract, models to account for long term deterioration of battery performance with age have been developed. Therefore, it will be advantageous to have precision battery cell performance data, identical to the precision tests described above, taken at intervals through the cell's life. This will provide the data needed to quantify the aging model being implemented. The aging process might then be expressed in terms of how the model parameters vary with time.

As well as supporting Watsun-PV model upgrading efforts, the short and long term battery test results will be of interest to many others with practical experience in battery installations.

## 9.4 PV-Diesel Model Application and Next Version

In addition to the battery work, it is reasonable to anticipate that the first version of the hybrid PV-diesel model now being developed will be followed quickly by a second version.

The PV-diesel hybrid model being developed and implemented in the current phase will be eventually exercised by Watsun and also Photron Canada, Howell-Mayhew, the client and other users. Being the first version of hybrid system modeling for Canadian applications, it can be anticipated that many valid improvements will be suggested as a natural evolution of the program. These improvements will involve realizations about the relative relevance of various model components and possibly even simplifications of the modeling concepts.

## References


1. Testing and Evaluation of Secondary Batteries for Use in Northern PV Installations (Phase II), J. Savage, O. Caporaletti, D. Heisler and S. Dixon, Ortech Int'l Final Report ETC/EDT-89-04, January, 1989.

2. Operational Experiences in Lead-Acid Batteries for PV Systems, B.L. Brench, 15th IEEE Photovoltaic Specialists Conference 642-47, 1981.

3. Field Tests of PV Power Systems, L.L. Bucciarelli, ISES Silver Jubilee, Atlanta, May-June 1979.

4. PVFORM - A New Approach To Photovoltaic System Performance Modeling, D.F. Menicucci, 18th IEEE Photovoltaic Specialists Conference 1614-19, 1985.

5. Low Power Photovoltaic Systems for Northern Applications, J. Savage, O. Caporaletti and R.W. Elliott, ORF Final Report ES/EPS-87-23, October 1987.

6. S. Singer, B. Rozenshtein and S. Surazi, Characterization of PV Array Output Using a Small Number of Measured Parameters, Solar Energy, 32, 5, 1984.

7. University of Wisconsin, TRNSYS, A Transient Simulation Program, Users Manual, Madison, Wisconsin, USA, December 1983.

8. E.A. Hyman, W.C. Spindler and J.F. Fatula, Phenomenological Discharge Voltage Model for Lead-Acid Batteries, Electrochemical Engineering Applications, AIChE Symposium Series, pp 78-86, 1986.

9. University of Waterloo, WATSUN-PV, User's Manual, Waterloo, Ontario.

10. Autonomous Photovoltaic-Diesel Power System Design, T.M. Calloway, 18th IEEE Photovoltaic Specialists Conference, p. 280-284, 1985.

11. G.W. Vinal, Storage Batteries, Wiley, New York, 1955, p. 244.

12. H. Bode, Lead Acid Storage Batteries, The Electrochemical Society Series, John Wiley and Sons.

13. K.V. Kordesch, ed., Batteries - Volume 2, Lead Acid Batteries and Electric Vehicles, Marcel Dekker Inc, New York, 1977.

14. D. Linden, Handbook of Batteries and Fuel Cells, McGraw-Hill, 1984.

15. Photovoltaic System Design Handbook, Prepared for the Ontario Ministry of Energy by Energy Resource Technologies Inc., Spectrum Engineering Ltd. and Mueller Associates Inc., Reference No. 681-8192, October 1984.